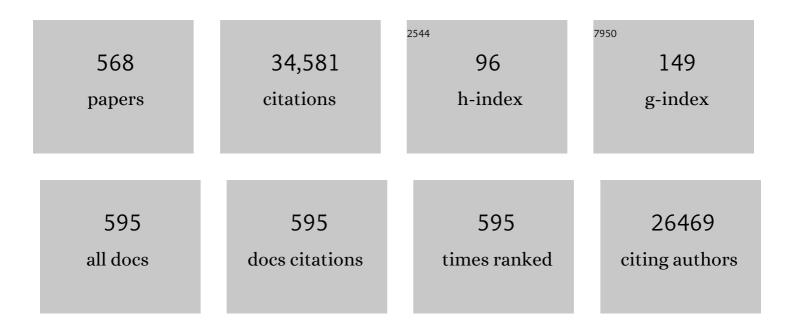
List of Publications by Year in descending order

Source: https://exaly.com/author-pdf/7063150/publications.pdf Version: 2024-02-01



EMIEL HENSEN

| # | Article | IF | CITATIONS |
|----|--|------|-----------|
| 1 | Engineering bunched Pt-Ni alloy nanocages for efficient oxygen reduction in practical fuel cells. Science, 2019, 366, 850-856. | 12.6 | 1,005 |
| 2 | Single-site trinuclear copper oxygen clusters in mordenite for selective conversion of methane to methanol. Nature Communications, 2015, 6, 7546. | 12.8 | 623 |
| 3 | Catalytic (de)hydrogenation promoted by non-precious metals – Co, Fe and Mn: recent advances in an emerging field. Chemical Society Reviews, 2018, 47, 1459-1483. | 38.1 | 511 |
| 4 | Highly Efficient and Robust Au/MgCuCr ₂ O ₄ Catalyst for Gas-Phase Oxidation of Ethanol to Acetaldehyde. Journal of the American Chemical Society, 2013, 135, 14032-14035. | 13.7 | 456 |
| 5 | Strategies for the Direct Catalytic Valorization of Methane Using Heterogeneous Catalysis: Challenges and Opportunities. ACS Catalysis, 2016, 6, 2965-2981. | 11.2 | 438 |
| 6 | Recent developments in zeolite membranes for gas separation. Journal of Membrane Science, 2016, 499, 65-79. | 8.2 | 435 |
| 7 | Heterogeneous and homogeneous catalysis for the hydrogenation of carboxylic acid derivatives: history, advances and future directions. Chemical Society Reviews, 2015, 44, 3808-3833. | 38.1 | 395 |
| 8 | The Relation between Morphology and Hydrotreating Activity for Supported MoS2 Particles. Journal of Catalysis, 2001, 199, 224-235. | 6.2 | 360 |
| 9 | Why Clays Swell. Journal of Physical Chemistry B, 2002, 106, 12664-12667. | 2.6 | 350 |
| 10 | Catalytic Depolymerization of Lignin in Supercritical Ethanol. ChemSusChem, 2014, 7, 2276-2288. | 6.8 | 313 |
| 11 | Tuning Pt-CeO2 interactions by high-temperature vapor-phase synthesis for improved reducibility of lattice oxygen. Nature Communications, 2019, 10, 1358. | 12.8 | 302 |
| 12 | Evaluating the Stability of Co ₂ P Electrocatalysts in the Hydrogen Evolution Reaction for Both Acidic and Alkaline Electrolytes. ACS Energy Letters, 2018, 3, 1360-1365. | 17.4 | 291 |
| 13 | Boosting CO2 hydrogenation via size-dependent metal–support interactions in cobalt/ceria-based catalysts. Nature Catalysis, 2020, 3, 526-533. | 34.4 | 286 |
| 14 | Highly Efficient Reversible Hydrogenation of Carbon Dioxide to Formates Using a Ruthenium PNPâ€₽incer Catalyst. ChemCatChem, 2014, 6, 1526-1530. | 3.7 | 283 |
| 15 | Complexity behind CO ₂ Capture on NH ₂ -MIL-53(Al). Langmuir, 2011, 27, 3970-3976. | 3.5 | 274 |
| 16 | Understanding the Anomalous Alkane Selectivity of ZIFâ€7 in the Separation of Light Alkane/Alkene Mixtures. Chemistry - A European Journal, 2011, 17, 8832-8840. | 3.3 | 274 |
| 17 | Ethanol as capping agent and formaldehyde scavenger for efficient depolymerization of lignin to aromatics. Green Chemistry, 2015, 17, 4941-4950. | 9.0 | 245 |
| 18 | Interface dynamics of Pd–CeO2 single-atom catalysts during CO oxidation. Nature Catalysis, 2021, 4, 469-478. | 34.4 | 244 |

| # | Article | IF | CITATIONS |
|----|--|------|-----------|
| 19 | Mechanism and microkinetics of the Fischer–Tropsch reaction. Physical Chemistry Chemical Physics, 2013, 15, 17038. | 2.8 | 233 |
| 20 | Engineering of Transition Metal Catalysts Confined in Zeolites. Chemistry of Materials, 2018, 30, 3177-3198. | 6.7 | 232 |
| 21 | CO oxidation by Pd supported on CeO2(100) and CeO2(111) facets. Applied Catalysis B: Environmental, 2019, 243, 36-46. | 20.2 | 231 |
| 22 | Mechanism of BrÃ,nsted acid-catalyzed conversion of carbohydrates. Journal of Catalysis, 2012, 295, 122-132. | 6.2 | 221 |
| 23 | Structure–performance descriptors and the role of Lewis acidity in the methanol-to-propylene process. Nature Chemistry, 2018, 10, 804-812. | 13.6 | 221 |
| 24 | Stability and reactivity of copper oxo-clusters in ZSM-5 zeolite for selective methane oxidation to methanol. Journal of Catalysis, 2016, 338, 305-312. | 6.2 | 217 |
| 25 | Phosphotungstic Acid Encapsulated in Metal–Organic Framework as Catalysts for Carbohydrate Dehydration to 5â€Hydroxymethylfurfural. ChemSusChem, 2011, 4, 59-64. | 6.8 | 216 |
| 26 | Structure and Reactivity of Zn-Modified ZSM-5 Zeolites: The Importance of Clustered Cationic Zn Complexes. ACS Catalysis, 2012, 2, 71-83. | 11.2 | 214 |
| 27 | The Optimally Performing Fischer–Tropsch Catalyst. Angewandte Chemie - International Edition, 2014, 53, 12746-12750. | 13.8 | 208 |
| 28 | Atomically Dispersed Pd–O Species on CeO ₂ (111) as Highly Active Sites for Low-Temperature CO Oxidation. ACS Catalysis, 2017, 7, 6887-6891. | 11.2 | 208 |
| 29 | Isolated Fe Sites in Metal Organic Frameworks Catalyze the Direct Conversion of Methane to Methanol. ACS Catalysis, 2018, 8, 5542-5548. | 11.2 | 200 |
| 30 | Effect of high-temperature treatment on Fe/ZSM-5 prepared by chemical vapor deposition of FeCl3I. Physicochemical characterization. Journal of Catalysis, 2004, 221, 560-574. | 6.2 | 192 |
| 31 | An in-situ IR study on the adsorption of CO2 and H2O on hydrotalcites. Journal of CO2 Utilization, 2018, 24, 228-239. | 6.8 | 183 |
| 32 | Ethanol dehydrogenation by gold catalysts: The effect of the gold particle size and the presence of oxygen. Applied Catalysis A: General, 2009, 361, 49-56. | 4.3 | 174 |
| 33 | On the deactivation of Mo/HZSM-5 in the methane dehydroaromatization reaction. Applied Catalysis B: Environmental, 2015, 176-177, 731-739. | 20.2 | 174 |
| 34 | Oxygen reduction reaction (ORR) activity and durability of carbon supported PtM (Co, Ni, Cu) alloys: Influence of particle size and non-noble metals. Applied Catalysis B: Environmental, 2012, 111-112, 515-526. | 20.2 | 170 |
| 35 | Hydrodeoxygenation of mono- and dimeric lignin model compounds on noble metal catalysts. Catalysis Today, 2014, 233, 83-91. | 4.4 | 170 |
| 36 | ZrO ₂ Is Preferred over TiO ₂ as Support for the Ru-Catalyzed Hydrogenation of Levulinic Acid to γ-Valerolactone. ACS Catalysis, 2016, 6, 5462-5472. | 11.2 | 169 |

| # | Article | IF | CITATIONS |
|----|--|------|-----------|
| 37 | Nonâ€Pincerâ€Type Manganese Complexes as Efficient Catalysts for the Hydrogenation of Esters. Angewandte Chemie - International Edition, 2017, 56, 7531-7534. | 13.8 | 169 |
| 38 | Molecular Simulations of Swelling Clay Minerals. Journal of Physical Chemistry B, 2004, 108, 7586-7596. | 2.6 | 168 |
| 39 | Influence of particle size on the activity and stability in steam methane reforming of supported Rh nanoparticles. Journal of Catalysis, 2011, 280, 206-220. | 6.2 | 166 |
| 40 | Role of Cu–Mg–Al Mixed Oxide Catalysts in Lignin Depolymerization in Supercritical Ethanol. ACS Catalysis, 2015, 5, 7359-7370. | 11.2 | 165 |
| 41 | Aerobic Oxidation of 5â€(Hydroxymethyl)furfural Cyclic Acetal Enables Selective Furanâ€2,5â€dicarboxylic Acid Formation with CeO ₂ â€Supported Gold Catalyst. Angewandte Chemie - International Edition, 2018, 57, 8235-8239. | 13.8 | 163 |
| 42 | Methane Dehydroaromatization by Mo/HZSM-5: Mono- or Bifunctional Catalysis?. ACS Catalysis, 2017, 7, 520-529. | 11.2 | 155 |
| 43 | Hysteresis in Clay Swelling Induced by Hydrogen Bonding:  Accurate Prediction of Swelling States. Langmuir, 2006, 22, 1223-1234. | 3.5 | 154 |
| 44 | Selective liquid phase hydrogenation of furfural to furfuryl alcohol by Ru/Zr-MOFs. Journal of Molecular Catalysis A, 2015, 406, 58-64. | 4.8 | 154 |
| 45 | Reductive fractionation of woody biomass into lignin monomers and cellulose by tandem metal triflate and Pd/C catalysis. Green Chemistry, 2017, 19, 175-187. | 9.0 | 154 |
| 46 | Formation of acid sites in amorphous silica-alumina. Journal of Catalysis, 2010, 269, 201-218. | 6.2 | 151 |
| 47 | Glucose Activation by Transient Cr ²⁺ Dimers. Angewandte Chemie - International Edition, 2010, 49, 2530-2534. | 13.8 | 150 |
| 48 | Influence of steaming on the acidity and the methanol conversion reaction of HZSM-5 zeolite. Journal of Catalysis, 2013, 307, 194-203. | 6.2 | 149 |
| 49 | SBA-15-supported nickel phosphide hydrotreating catalysts. Journal of Catalysis, 2008, 253, 119-131. | 6.2 | 148 |
| 50 | Stable Mo/HZSM-5 methane dehydroaromatization catalysts optimized for high-temperature calcination-regeneration. Journal of Catalysis, 2017, 346, 125-133. | 6.2 | 147 |
| 51 | Promotional effect of transition metal doping on the basicity and activity of calcined hydrotalcite catalysts for glycerol carbonate synthesis. Applied Catalysis B: Environmental, 2014, 144, 135-143. | 20.2 | 146 |
| 52 | Characterization and reactivity of Ga+ and GaO+ cations in zeolite ZSM-5. Journal of Catalysis, 2006, 239, 478-485. | 6.2 | 145 |
| 53 | Mesoporous SSZ-13 zeolite prepared by a dual-template method with improved performance in the methanol-to-olefins reaction. Journal of Catalysis, 2013, 298, 27-40. | 6.2 | 144 |
| 54 | High flux high-silica SSZ-13 membrane for CO ₂ separation. Journal of Materials Chemistry A. 2014, 2, 13083-13092. | 10.3 | 142 |

| # | Article | IF | CITATIONS |
|----|---|------|-----------|
| 55 | Highly Active and Recyclable Snâ€MWW Zeolite Catalyst for Sugar Conversion to Methyl Lactate and Lactic Acid. ChemSusChem, 2013, 6, 1352-1356. | 6.8 | 140 |
| 56 | The impact of Metal–Ligand Cooperation in Hydrogenation of Carbon Dioxide Catalyzed by Ruthenium PNP Pincer. ACS Catalysis, 2013, 3, 2522-2526. | 11.2 | 136 |
| 57 | Exposed Surfaces on Shapeâ€Controlled Ceria Nanoparticles Revealed through ACâ€TEM and Water–Gas Shift Reactivity. ChemSusChem, 2013, 6, 1898-1906. | 6.8 | 134 |
| 58 | Enhanced Catalytic Oxidation by Hierarchically Structured TS-1 Zeolite. Journal of Physical Chemistry C, 2010, 114, 6553-6559. | 3.1 | 133 |
| 59 | Optimum Cu nanoparticle catalysts for CO2 hydrogenation towards methanol. Nano Energy, 2018, 43, 200-209. | 16.0 | 133 |
| 60 | Acidity Characterization of Amorphous Silica–Alumina. Journal of Physical Chemistry C, 2012, 116, 21416-21429. | 3.1 | 129 |
| 61 | Confined Carbon Mediating Dehydroaromatization of Methane over Mo/ZSMâ€5. Angewandte Chemie - International Edition, 2018, 57, 1016-1020. | 13.8 | 128 |
| 62 | On the activity of supported Au catalysts in the liquid phase hydrogenation of CO2 to formates. Journal of Catalysis, 2016, 343, 97-105. | 6.2 | 126 |
| 63 | A Linear Scaling Relation for CO Oxidation on CeO ₂ -Supported Pd. Journal of the American Chemical Society, 2018, 140, 4580-4587. | 13.7 | 126 |
| 64 | Synthesis of stable and low-CO ₂ selective Îμ-iron carbide Fischer-Tropsch catalysts. Science Advances, 2018, 4, eaau2947. | 10.3 | 126 |
| 65 | Chemistry of N2O decomposition on active sites with different nature: Effect of high-temperature treatment of Fe/ZSM-5. Journal of Catalysis, 2006, 238, 186-195. | 6.2 | 125 |
| 66 | First-Principles-Based Microkinetics Simulations of Synthesis Gas Conversion on a Stepped Rhodium Surface. ACS Catalysis, 2015, 5, 5453-5467. | 11.2 | 124 |
| 67 | Efficient Base-Metal NiMn/TiO ₂ Catalyst for CO ₂ Methanation. ACS Catalysis, 2019, 9, 7823-7839. | 11.2 | 124 |
| 68 | Understanding carbon dioxide activation and carbon–carbon coupling over nickel. Nature Communications, 2019, 10, 5330. | 12.8 | 124 |
| 69 | Extraframework Feî—,Alî—,O species occluded in MFI zeolite as the active species in the oxidation of benzene to phenol with nitrous oxide. Journal of Catalysis, 2003, 220, 260-264. | 6.2 | 122 |
| 70 | The Mechanism of Glucose Isomerization to Fructose over Snâ€BEA Zeolite: A Periodic Density Functional Theory Study. ChemSusChem, 2013, 6, 1688-1696. | 6.8 | 122 |
| 71 | Direct NO and N2O decomposition and NO-assisted N2O decomposition over Cu-zeolites: Elucidating the influence of the CuCu distance on oxygen migration. Journal of Catalysis, 2007, 245, 358-368. | 6.2 | 120 |
| 72 | Mechanistic Aspects of the Water–Gas Shift Reaction on Isolated and Clustered Au Atoms on CeO ₂ (110): A Density Functional Theory Study. ACS Catalysis, 2014, 4, 1885-1892. | 11.2 | 120 |

| # | Article | IF | CITATIONS |
|----|---|------|-----------|
| 73 | Synergy between Lewis acid sites and hydroxyl groups for the isomerization of glucose to fructose over Sn-containing zeolites: a theoretical perspective. Catalysis Science and Technology, 2014, 4, 2241-2250. | 4.1 | 117 |
| 74 | Trimodal Porous Hierarchical SSZ-13 Zeolite with Improved Catalytic Performance in the Methanol-to-Olefins Reaction. ACS Catalysis, 2016, 6, 2163-2177. | 11.2 | 116 |
| 75 | Effect of high-temperature treatment on Fe/ZSM-5 prepared by chemical vapor deposition of FeCl3II. Nitrous oxide decomposition, selective oxidation of benzene to phenol, and selective reduction of nitric oxide by isobutane. Journal of Catalysis, 2004, 221, 575-583. | 6.2 | 112 |
| 76 | Dual template synthesis of a highly mesoporous SSZ-13 zeolite with improved stability in the methanol-to-olefins reaction. Chemical Communications, 2012, 48, 9492. | 4.1 | 112 |
| 77 | Mechanism of CO ₂ hydrogenation to formates by homogeneous Ru-PNP pincer catalyst: from a theoretical description to performance optimization. Catalysis Science and Technology, 2014, 4, 3474-3485. | 4.1 | 112 |
| 78 | Temperature-Dependent Kinetic Studies of the Chlorine Evolution Reaction over RuO ₂ (110) Model Electrodes. ACS Catalysis, 2017, 7, 2403-2411. | 11.2 | 111 |
| 79 | Stable Pd-Doped Ceria Structures for CH ₄ Activation and CO Oxidation. ACS Catalysis, 2018, 8, 75-80. | 11.2 | 111 |
| 80 | A Tensileâ€Strained Pt–Rh Singleâ€Atom Alloy Remarkably Boosts Ethanol Oxidation. Advanced Materials, 2021, 33, e2008508. | 21.0 | 111 |
| 81 | Defect Chemistry of Ceria Nanorods. Journal of Physical Chemistry C, 2014, 118, 4131-4142. | 3.1 | 110 |
| 82 | A model compound (methyl oleate, oleic acid, triolein) study of triglycerides hydrodeoxygenation over alumina-supported NiMo sulfide. Applied Catalysis B: Environmental, 2017, 201, 290-301. | 20.2 | 110 |
| 83 | Molecular Aspects of Glucose Dehydration by Chromium Chlorides in Ionic Liquids. Chemistry - A European Journal, 2011, 17, 5281-5288. | 3.3 | 109 |
| 84 | Catalytic Hydrogenation of CO ₂ to Formates by a Lutidine-Derived Ru–CNC Pincer Complex: Theoretical Insight into the Unrealized Potential. ACS Catalysis, 2015, 5, 1145-1154. | 11.2 | 109 |
| 85 | A hierarchical Fe/ZSM-5 zeolite with superior catalytic performance for benzene hydroxylation to phenol. Chemical Communications, 2009, , 7590. | 4.1 | 106 |
| 86 | The Effect of Support Interaction on the Sulfidability of Al2O3- and TiO2-Supported CoW and NiW Hydrodesulfurization Catalysts. Journal of Catalysis, 2001, 198, 151-163. | 6.2 | 105 |
| 87 | Nature and Location of Cationic Lanthanum Species in High Alumina Containing Faujasite Type Zeolites. Journal of Physical Chemistry C, 2011, 115, 21763-21776. | 3.1 | 105 |
| 88 | Synthesis of Snâ€Beta with Exclusive and High Framework Sn Content. ChemCatChem, 2015, 7, 1152-1160. | 3.7 | 105 |
| 89 | A Refinement on the Notion of Type I and II (Co)MoS Phases in Hydrotreating Catalysts. Catalysis Letters, 2002, 84, 59-67. | 2.6 | 104 |
| 90 | Lutidine-Derived Ru-CNC Hydrogenation Pincer Catalysts with Versatile Coordination Properties. ACS Catalysis, 2014, 4, 2667-2671. | 11.2 | 104 |

| # | Article | IF | CITATIONS |
|-----|--|------|-----------|
| 91 | Pt-Re synergy in aqueous-phase reforming of glycerol and the water–gas shift reaction. Journal of Catalysis, 2014, 311, 88-101. | 6.2 | 103 |
| 92 | Effective Release of Lignin Fragments from Lignocellulose by Lewis Acid Metal Triflates in the Ligninâ€First Approach. ChemSusChem, 2016, 9, 3262-3267. | 6.8 | 103 |
| 93 | Adsorption isotherms of water in Li–, Na–, and K–montmorillonite by molecular simulation. Journal of Chemical Physics, 2001, 115, 3322-3329. | 3.0 | 102 |
| 94 | Structure–Activity Correlations in Hydrodesulfurization Reactions over Ni-Promoted Mo _{<i>x</i>} W _(1–<i>x</i>) S ₂ /Al ₂ O ₃ Catalysts. ACS Catalysis, 2015, 5, 7276-7287. | 11.2 | 101 |
| 95 | Theoretical Approach To Predict the Stability of Supported Single-Atom Catalysts. ACS Catalysis, 2019, 9, 3289-3297. | 11.2 | 101 |
| 96 | A comprehensive density functional theory study of ethane dehydrogenation over reduced extra-framework gallium species in ZSM-5 zeolite. Journal of Catalysis, 2006, 240, 73-84. | 6.2 | 99 |
| 97 | On two alternative mechanisms of ethane activation over ZSM-5 zeolite modified by Zn2+ and Ga1+ cations. Physical Chemistry Chemical Physics, 2005, 7, 3088. | 2.8 | 98 |
| 98 | Influence of Extraframework Aluminum on the BrÃ,nsted Acidity and Catalytic Reactivity of Faujasite Zeolite. ChemCatChem, 2013, 5, 452-466. | 3.7 | 98 |
| 99 | Structure, Stability, and Lewis Acidity of Mono and Double Ti, Zr, and Sn Framework Substitutions in BEA Zeolites: A Periodic Density Functional Theory Study. Journal of Physical Chemistry C, 2013, 117, 3976-3986. | 3.1 | 98 |
| 100 | Influence of the Si/Al ratio on the separation properties of SSZ-13 zeolite membranes. Journal of Membrane Science, 2015, 484, 140-145. | 8.2 | 98 |
| 101 | Synthesis of glycerol carbonate by transesterification of glycerol with dimethyl carbonate over MgAl mixed oxide catalysts. Applied Catalysis A: General, 2013, 467, 124-131. | 4.3 | 97 |
| 102 | Stable Fe/ZSM-5 Nanosheet Zeolite Catalysts for the Oxidation of Benzene to Phenol. ACS Catalysis, 2017, 7, 2709-2719. | 11.2 | 96 |
| 103 | Ex Situ and Operando Studies on the Role of Copper in Cu-Promoted SiO ₂ –MgO Catalysts for the Lebedev Ethanol-to-Butadiene Process. ACS Catalysis, 2015, 5, 6005-6015. | 11.2 | 95 |
| 104 | Selective Coke Combustion by Oxygen Pulsing During Mo/ZSMâ€5â€Catalyzed Methane Dehydroaromatization. Angewandte Chemie - International Edition, 2016, 55, 15086-15090. | 13.8 | 94 |
| 105 | Mechanism of Cobalt-Catalyzed CO Hydrogenation: 2. Fischer–Tropsch Synthesis. ACS Catalysis, 2017, 7, 8061-8071. | 11.2 | 94 |
| 106 | Supported Rhodium Oxide Nanoparticles as Highly Active CO Oxidation Catalysts. Angewandte Chemie - International Edition, 2011, 50, 5306-5310. | 13.8 | 93 |
| 107 | Efficient Tandem Synthesis of Methyl Esters and Imines by Using Versatile Hydrotalcite upported Gold Nanoparticles. Chemistry - A European Journal, 2012, 18, 12122-12129. | 3.3 | 93 |
| 108 | Nature and Catalytic Role of Extraframework Aluminum in Faujasite Zeolite: A Theoretical Perspective. ACS Catalysis, 2015, 5, 7024-7033. | 11.2 | 92 |

| # | Article | IF | CITATIONS |
|-----|---|------|-----------|
| 109 | Mechanism and Nature of Active Sites for Methanol Synthesis from CO/CO ₂ on Cu/CeO ₂ . ACS Catalysis, 2020, 10, 11532-11544. | 11.2 | 92 |
| 110 | N2O Decomposition over Fe/ZSM-5: Effect of High-Temperature Calcination and Steaming. Catalysis Letters, 2002, 81, 205-212. | 2.6 | 90 |
| 111 | Aerobic oxidation of alcohols over hydrotalcite-supported gold nanoparticles: the promotional effect of transition metal cations. Chemical Communications, 2011, 47, 11540. | 4.1 | 90 |
| 112 | Dehydration of Different Ketoses and Aldoses to 5â€Hydroxymethylfurfural. ChemSusChem, 2013, 6, 1681-1687. | 6.8 | 90 |
| 113 | Bis-N-heterocyclic Carbene Aminopincer Ligands Enable High Activity in Ru-Catalyzed Ester Hydrogenation. Journal of the American Chemical Society, 2015, 137, 7620-7623. | 13.7 | 90 |
| 114 | Highly Active and Stable CH ₄ Oxidation by Substitution of Ce ⁴⁺ by Two Pd ²⁺ lons in CeO ₂ (111). ACS Catalysis, 2018, 8, 6552-6559. | 11.2 | 90 |
| 115 | The Origin of High Activity of Amorphous MoS ₂ in the Hydrogen Evolution Reaction. ChemSusChem, 2019, 12, 4383-4389. | 6.8 | 90 |
| 116 | Cracking of n-heptane over BrÃ,nsted acid sites and Lewis acid Ga sites in ZSM-5 zeolite. Microporous and Mesoporous Materials, 2008, 110, 279-291. | 4.4 | 89 |
| 117 | Dehydrogenation of Light Alkanes over Isolated Gallyl Ions in Ga/ZSM-5 Zeolites. Journal of Physical Chemistry C, 2007, 111, 13068-13075. | 3.1 | 87 |
| 118 | Catalytic performance of sheet-like Fe/ZSM-5 zeolites for the selective oxidation of benzene with nitrous oxide. Journal of Catalysis, 2013, 299, 81-89. | 6.2 | 87 |
| 119 | Lewis-acid catalyzed depolymerization of Protobind lignin in supercritical water and ethanol. Catalysis Today, 2016, 259, 460-466. | 4.4 | 87 |
| 120 | Particle Size and Crystal Phase Effects in Fischer-Tropsch Catalysts. Engineering, 2017, 3, 467-476. | 6.7 | 87 |
| 121 | One-Step Synthesis of Hierarchical ZSM-5 Using Cetyltrimethylammonium as Mesoporogen and Structure-Directing Agent. Chemistry of Materials, 2017, 29, 4091-4096. | 6.7 | 86 |
| 122 | Reactivity, Selectivity, and Stability of Zeoliteâ€Based Catalysts for Methane Dehydroaromatization. Advanced Materials, 2020, 32, e2002565. | 21.0 | 86 |
| 123 | Periodic Trends in Hydrotreating Catalysis: Thiophene Hydrodesulfurization over Carbon-Supported 4d Transition Metal Sulfides. Journal of Catalysis, 2000, 192, 98-107. | 6.2 | 85 |
| 124 | Insight into the formation of the active phases in supported NiW hydrotreating catalysts. Applied Catalysis A: General, 2007, 322, 16-32. | 4.3 | 85 |
| 125 | Simultaneous NO _{<i>x</i>} and Particulate Matter Removal from Diesel Exhaust by Hierarchical Fe-Doped Ce–Zr Oxide. ACS Catalysis, 2017, 7, 3883-3892. | 11.2 | 85 |
| 126 | Catalytic Depolymerization of Lignin and Woody Biomass in Supercritical Ethanol: Influence of Reaction Temperature and Feedstock. ACS Sustainable Chemistry and Engineering, 2017, 5, 10864-10874. | 6.7 | 84 |

| # | Article | IF | CITATIONS |
|-----|---|------|-----------|
| 127 | Role of Adsorbed Water on Charge Carrier Dynamics in Photoexcited TiO ₂ . Journal of Physical Chemistry C, 2017, 121, 7514-7524. | 3.1 | 82 |
| 128 | Selective Production of Biobased Phenol from Lignocellulose-Derived Alkylmethoxyphenols. ACS Catalysis, 2018, 8, 11184-11190. | 11.2 | 82 |
| 129 | Catalytic Conversion of Lignin in Woody Biomass into Phenolic Monomers in Methanol/Water Mixtures without External Hydrogen. ACS Sustainable Chemistry and Engineering, 2019, 7, 13764-13773. | 6.7 | 82 |
| 130 | Structure and Evolution of Confined Carbon Species during Methane Dehydroaromatization over Mo/ZSM-5. ACS Catalysis, 2018, 8, 8459-8467. | 11.2 | 79 |
| 131 | Ni–In Synergy in CO ₂ Hydrogenation to Methanol. ACS Catalysis, 2021, 11, 11371-11384. | 11.2 | 79 |
| 132 | Waterâ€Promoted Hydrocarbon Activation Catalyzed by Binuclear Gallium Sites in ZSMâ€5 Zeolite. Angewandte Chemie - International Edition, 2007, 46, 7273-7276. | 13.8 | 78 |
| 133 | Increased activity in the oxygen evolution reaction by Fe ⁴⁺ -induced hole states in perovskite La _{1â^'x} Sr _x FeO ₃ . Journal of Materials Chemistry A, 2020, 8, 4407-4415. | 10.3 | 78 |
| 134 | Ni ³⁺ -Induced Hole States Enhance the Oxygen Evolution Reaction Activity of Ni _{<i>x</i>} Co _{3–<i>x</i>} O ₄ Electrocatalysts. Chemistry of Materials, 2019, 31, 7618-7625. | 6.7 | 76 |
| 135 | Stability of Extraframework Iron-Containing Complexes in ZSM-5 Zeolite. Journal of Physical Chemistry C, 2013, 117, 413-426. | 3.1 | 75 |
| 136 | Hierarchically structured Fe/ZSM-5 as catalysts for the oxidation of benzene to phenol. Microporous and Mesoporous Materials, 2011, 145, 172-181. | 4.4 | 74 |
| 137 | Scaling Relations for Acidity and Reactivity of Zeolites. Journal of Physical Chemistry C, 2017, 121, 23520-23530. | 3.1 | 74 |
| 138 | Electronic Structure of the [Cu ₃ (μ-O) ₃] ²⁺ Cluster in Mordenite Zeolite and Its Effects on the Methane to Methanol Oxidation. Journal of Physical Chemistry C, 2017, 121, 22295-22302. | 3.1 | 74 |
| 139 | Coupling organosolv fractionation and reductive depolymerization of woody biomass in a two-step catalytic process. Green Chemistry, 2018, 20, 2308-2319. | 9.0 | 74 |
| 140 | Hydrodeoxygenation of guaiacol over Ni2P/SiO2–reaction mechanism and catalyst deactivation. Applied Catalysis A: General, 2018, 550, 57-66. | 4.3 | 74 |
| 141 | In situ Ga K edge XANES study of the activation of Ga/ZSM-5 prepared by chemical vapor deposition of trimethylgallium. Catalysis Letters, 2005, 101, 79-85. | 2.6 | 73 |
| 142 | Gold Stabilized by Nanostructured Ceria Supports: Nature of the Active Sites and Catalytic Performance. Topics in Catalysis, 2011, 54, 424-438. | 2.8 | 73 |
| 143 | Self-organization of extraframework cations in zeolites. Proceedings of the Royal Society A: Mathematical, Physical and Engineering Sciences, 2012, 468, 2070-2086. | 2.1 | 73 |
| 144 | Influence of sulfiding agent and pressure on structure and performance of CoMo/Al2O3 hydrodesulfurization catalysts. Journal of Catalysis, 2016, 342, 27-39. | 6.2 | 73 |

| # | Article | IF | CITATIONS |
|-----|---|------|-----------|
| 145 | Flame Synthesis of Cu/ZnO–CeO ₂ Catalysts: Synergistic Metal–Support Interactions Promote CH ₃ OH Selectivity in CO ₂ Hydrogenation. ACS Catalysis, 2021, 11, 4880-4892. | 11.2 | 73 |
| 146 | Cu2O photoelectrodes for solar water splitting: Tuning photoelectrochemical performance by controlled faceting. Solar Energy Materials and Solar Cells, 2015, 141, 178-186. | 6.2 | 72 |
| 147 | Relationship between acidity and catalytic reactivity of faujasite zeolite: A periodic DFT study. Journal of Catalysis, 2016, 344, 570-577. | 6.2 | 72 |
| 148 | Support effects in the aqueous phase reforming of glycerol over supported platinum catalysts. Applied Catalysis A: General, 2012, 431-432, 113-119. | 4.3 | 71 |
| 149 | Grand challenges for catalysis in the Science and Technology Roadmap on Catalysis for Europe: moving ahead for a sustainable future. Catalysis Science and Technology, 2017, 7, 5182-5194. | 4.1 | 71 |
| 150 | Aqueous phase reforming of glycerol over Re-promoted Pt and Rh catalysts. Green Chemistry, 2014, 16, 853-863. | 9.0 | 70 |
| 151 | The effect of organic additives and phosphoric acid on sulfidation and activity of (Co)Mo/Al2O3 hydrodesulfurization catalysts. Journal of Catalysis, 2017, 351, 95-106. | 6.2 | 70 |
| 152 | Ni-Mn catalysts on silica-modified alumina for CO2 methanation. Journal of Catalysis, 2020, 382, 358-371. | 6.2 | 70 |
| 153 | Aromatization of ethylene over zeolite-based catalysts. Catalysis Science and Technology, 2020, 10, 2774-2785. | 4.1 | 70 |
| 154 | Effect of Aluminum on the Nature of the Iron Species in Fe-SBA-15. Journal of Physical Chemistry B, 2006, 110, 26114-26121. | 2.6 | 69 |
| 155 | Stability and reactivity of active sites for direct benzene oxidation to phenol in Fe/ZSM-5: A comprehensive periodic DFT study. Journal of Catalysis, 2011, 284, 194-206. | 6.2 | 69 |
| 156 | BrÃ,nsted acidity of Al/SBA-15. Microporous and Mesoporous Materials, 2012, 151, 34-43. | 4.4 | 69 |
| 157 | Highâ€Efficiency InPâ€Based Photocathode for Hydrogen Production by Interface Energetics Design and Photon Management. Advanced Functional Materials, 2016, 26, 679-686. | 14.9 | 69 |
| 158 | Selective production of mono-aromatics from lignocellulose over Pd/C catalyst: the influence of acid co-catalysts. Faraday Discussions, 2017, 202, 141-156. | 3.2 | 69 |
| 159 | N-formyl-stabilizing quasi-catalytic species afford rapid and selective solvent-free amination of biomass-derived feedstocks. Nature Communications, 2019, 10, 699. | 12.8 | 69 |
| 160 | Title is missing!. Catalysis Letters, 2003, 86, 25-31. | 2.6 | 68 |
| 161 | Gallium-promoted HZSM-5 zeolites as efficient catalysts for the aromatization of biomass-derived furans. Chemical Engineering Science, 2019, 198, 305-316. | 3.8 | 68 |
| 162 | Porous MOFs supported palladium catalysts for phenol hydrogenation: A comparative study on MIL-101 and MIL-53. Catalysis Communications, 2013, 41, 47-51. | 3.3 | 67 |

| # | Article | IF | CITATIONS |
|-----|--|------|-----------|
| 163 | Influence of Rh nanoparticle size and composition on the photocatalytic water splitting performance of Rh/graphitic carbon nitride. International Journal of Hydrogen Energy, 2014, 39, 11537-11546. | 7.1 | 67 |
| 164 | Theory of surface chemistry and reactivity of reducible oxides. Catalysis Today, 2015, 244, 63-84. | 4.4 | 67 |
| 165 | Theoretical Study of Ripening Mechanisms of Pd Clusters on Ceria. Chemistry of Materials, 2017, 29, 9456-9462. | 6.7 | 67 |
| 166 | Elucidating the electronic structure of CuWO ₄ thin films for enhanced photoelectrochemical water splitting. Journal of Materials Chemistry A, 2019, 7, 11895-11907. | 10.3 | 67 |
| 167 | DRIFTS study of the nature and chemical reactivity of gallium ions in Ga/ZSM-5II. Oxidation of reduced Ga species in ZSM-5 by nitrous oxide or water. Journal of Catalysis, 2005, 233, 351-358. | 6.2 | 66 |
| 168 | On the Mechanism of Lewis Acid Catalyzed Glucose Transformations in Ionic Liquids. ChemCatChem, 2012, 4, 1263-1271. | 3.7 | 66 |
| 169 | Enhancement of Catalyst Performance in the Direct Propene Epoxidation: A Study into Gold–Titanium Synergy. ChemCatChem, 2013, 5, 467-478. | 3.7 | 66 |
| 170 | Desilication and silylation of Mo/HZSM-5 for methane dehydroaromatization. Microporous and Mesoporous Materials, 2015, 203, 259-273. | 4.4 | 66 |
| 171 | A dual-templating synthesis strategy to hierarchical ZSM-5 zeolites as efficient catalysts for the methanol-to-hydrocarbons reaction. Journal of Catalysis, 2018, 361, 135-142. | 6.2 | 66 |
| 172 | BrÃ,nsted acid sites of zeolitic strength in amorphous silica-alumina. Chemical Communications, 2010, 46, 3466. | 4.1 | 65 |
| 173 | Reversible Nature of Coke Formation on Mo/ZSMâ€5 Methane Dehydroaromatization Catalysts. Angewandte Chemie - International Edition, 2019, 58, 7068-7072. | 13.8 | 65 |
| 174 | Quantification of Strong BrÃ,nsted Acid Sites in Aluminosilicates. Journal of Physical Chemistry C, 2010, 114, 8363-8374. | 3.1 | 64 |
| 175 | Surface-Dependence of Defect Chemistry of Nanostructured Ceria. Journal of Physical Chemistry C, 2015, 119, 12423-12433. | 3.1 | 64 |
| 176 | Dehydration of Glucose to 5â€Hydroxymethylfurfural Using Nbâ€doped Tungstite. ChemSusChem, 2016, 9, 2421-2429. | 6.8 | 64 |
| 177 | Enhanced Photoresponse of FeS ₂ Films: The Role of Marcasite–Pyrite Phase Junctions. Advanced Materials, 2016, 28, 9602-9607. | 21.0 | 64 |
| 178 | Kinetics and Mechanism of Thiophene Hydrodesulfurization over Carbon-Supported Transition Metal Sulfides. Journal of Catalysis, 1996, 163, 429-435. | 6.2 | 63 |
| 179 | Comparison of mesoporous SSZ-13 and SAPO-34 zeolite catalysts for the methanol-to-olefins reaction. Catalysis Today, 2014, 235, 160-168. | 4.4 | 63 |
| 180 | On the role of aluminum in the selective oxidation of benzene to phenol by nitrous oxide over iron-containing MFI zeolites: an in situ Fe XANES study. Journal of Catalysis, 2004, 226, 466-470. | 6.2 | 61 |

| # | Article | IF | CITATIONS |
|-----|---|------|-----------|
| 181 | Coordination Properties of Ionic Liquid-Mediated Chromium(II) and Copper(II) Chlorides and Their Complexes with Glucose. Inorganic Chemistry, 2010, 49, 10081-10091. | 4.0 | 61 |
| 182 | Influence of Carbon Deposits on the Cobalt-Catalyzed Fischer–Tropsch Reaction: Evidence of a Two-Site Reaction Model. ACS Catalysis, 2018, 8, 1580-1590. | 11.2 | 61 |
| 183 | Hierarchical zeolites prepared by organosilane templating: A study of the synthesis mechanism and catalytic activity. Catalysis Today, 2011, 168, 96-111. | 4.4 | 60 |
| 184 | A computational DFT study of CO oxidation on a Au nanorod supported on CeO2(110): on the role of the support termination. Catalysis Science and Technology, 2013, 3, 3020. | 4.1 | 60 |
| 185 | Enhancing the electrocatalytic activity of 2H-WS ₂ for hydrogen evolution <i>via</i> defect engineering. Physical Chemistry Chemical Physics, 2019, 21, 6071-6079. | 2.8 | 60 |
| 186 | Towards a Selective Heterogeneous Catalyst for Glucose Dehydration to 5â€Hydroxymethylfurfural in Water: CrCl ₂ Catalysis in a Thin Immobilized Ionic Liquid Layer. ChemCatChem, 2011, 3, 969-972. | 3.7 | 58 |
| 187 | Facile synthesis of the DD3R zeolite: performance in the adsorptive separation of buta-1,3-diene and but-2-ene isomers. Journal of Materials Chemistry, 2011, 21, 18386. | 6.7 | 57 |
| 188 | Unraveling the synergy between gold nanoparticles and chromium-hydrotalcites in aerobic oxidation of alcohols. Journal of Catalysis, 2014, 313, 80-91. | 6.2 | 57 |
| 189 | A DFT Study of CO Oxidation at the Pd–CeO ₂ (110) Interface. Journal of Physical Chemistry C, 2015, 119, 27505-27511. | 3.1 | 57 |
| 190 | Temperature-programmed plasma surface reaction: An approach to determine plasma-catalytic performance. Applied Catalysis B: Environmental, 2018, 239, 168-177. | 20.2 | 57 |
| 191 | Hydrogenation of levulinic acid to ^ĵ -valerolactone over Fe-Re/TiO2 catalysts. Applied Catalysis B: Environmental, 2020, 278, 119314. | 20.2 | 57 |
| 192 | On the synthesis of highly acidic nanolayered ZSM-5. Journal of Catalysis, 2015, 327, 10-21. | 6.2 | 56 |
| 193 | On the influence of steam on the CO2 chemisorption capacity of a hydrotalcite-based adsorbent for SEWGS applications. Chemical Engineering Journal, 2017, 314, 554-569. | 12.7 | 56 |
| 194 | Kinetics of the Fischer–Tropsch Reaction. Angewandte Chemie - International Edition, 2012, 51, 9015-9019. | 13.8 | 55 |
| 195 | Selective oxidation of ethanol to acetaldehyde by Auâ^'Ir catalysts. Journal of Catalysis, 2013, 305, 135-145. | 6.2 | 55 |
| 196 | Monomer Formation Model versus Chain Growth Model of the Fischer–Tropsch Reaction. Journal of Physical Chemistry C, 2013, 117, 4488-4504. | 3.1 | 55 |
| 197 | A mechanistic DFT study of low temperature SCR of NO with NH ₃ on MnCe _{1â^'x} O ₂ (111). Catalysis Science and Technology, 2016, 6, 2120-2128. | 4.1 | 55 |
| 198 | Highly stable Pt ₃ Ni nanowires tailored with trace Au for the oxygen reduction reaction. Journal of Materials Chemistry A, 2019, 7, 26402-26409. | 10.3 | 55 |

| # | Article | IF | CITATIONS |
|-----|---|------|-----------|
| 199 | Sulfated Zirconia Modified SBA-15 Catalysts for Cellobiose Hydrolysis. Catalysis Letters, 2011, 141, 33-42. | 2.6 | 54 |
| 200 | Nanostructured ceria supported Pt and Au catalysts for the reactions of ethanol and formic acid. Applied Catalysis B: Environmental, 2013, 130-131, 325-335. | 20.2 | 54 |
| 201 | Chemisorption working capacity and kinetics of CO 2 and H 2 O of hydrotalcite-based adsorbents for sorption-enhanced water-gas-shift applications. Chemical Engineering Journal, 2016, 293, 9-23. | 12.7 | 54 |
| 202 | An Active Alkali-Exchanged Faujasite Catalyst for <i>p</i> -Xylene Production via the One-Pot Diels–Alder Cycloaddition/Dehydration Reaction of 2,5-Dimethylfuran with Ethylene. ACS Catalysis, 2018, 8, 760-769. | 11.2 | 54 |
| 203 | Mechanism of Cobalt-Catalyzed CO Hydrogenation: 1. Methanation. ACS Catalysis, 2017, 7, 8050-8060. | 11.2 | 53 |
| 204 | Mn promotion of rutile TiO2-RuO2 anodes for water oxidation in acidic media. Applied Catalysis B: Environmental, 2020, 261, 118225. | 20.2 | 53 |
| 205 | Basic metal carbonate supported gold nanoparticles: enhanced performance in aerobic alcohol oxidation. Green Chemistry, 2009, 11, 322. | 9.0 | 52 |
| 206 | Influence of steam-calcination and acid leaching treatment on the VGO hydrocracking performance of faujasite zeolite. Fuel Processing Technology, 2015, 133, 89-96. | 7.2 | 52 |
| 207 | Charge Transport over the Defective CeO ₂ (111) Surface. Chemistry of Materials, 2016, 28, 5652-5658. | 6.7 | 52 |
| 208 | Quantum chemistry of the Fischer–Tropsch reaction catalysed by a stepped ruthenium surface. Catalysis Science and Technology, 2014, 4, 3129-3140. | 4.1 | 51 |
| 209 | Lewis acid-catalyzed depolymerization of soda lignin in supercritical ethanol/water mixtures. Catalysis Today, 2016, 269, 9-20. | 4.4 | 51 |
| 210 | Effective Strategy for High-Yield Furan Dicarboxylate Production for Biobased Polyester Applications. ACS Catalysis, 2019, 9, 4277-4285. | 11.2 | 51 |
| 211 | Hydrogen–Deuterium Equilibration over Transition Metal Sulfide Catalysts: On the Synergetic Effect in CoMo Catalysts. Journal of Catalysis, 1999, 187, 95-108. | 6.2 | 50 |
| 212 | Multinuclear gallium-oxide cations in high-silica zeolites. Physical Chemistry Chemical Physics, 2009, 11, 2893. | 2.8 | 50 |
| 213 | MoO ₃ –TiO ₂ synergy in oxidative dehydrogenation of lactic acid to pyruvic acid. Green Chemistry, 2017, 19, 3014-3022. | 9.0 | 50 |
| 214 | Effects of the Functionalization of the Ordered Mesoporous Carbon Support Surface on Iron Catalysts for the Fischer–Tropsch Synthesis of Lower Olefins. ChemCatChem, 2017, 9, 620-628. | 3.7 | 50 |
| 215 | Correlations between Density-Based Bond Orders and Orbital-Based Bond Energies for Chemical Bonding Analysis. Journal of Physical Chemistry C, 2019, 123, 2843-2854. | 3.1 | 50 |
| 216 | Selective hydrogenation of 5-hydroxymethylfurfural and its acetal with 1,3-propanediol to 2,5-bis(hydroxymethyl)furan using supported rhenium-promoted nickel catalysts in water. Green Chemistry, 2020, 22, 1229-1238. | 9.0 | 50 |

| # | Article | IF | CITATIONS |
|-----|---|-----------|-----------|
| 217 | Unfolding and Mechanochemical Scission of Supramolecular Polymers Containing a Metal–Ligand Coordination Bond. Macromolecules, 2011, 44, 9187-9195. | 4.8 | 49 |
| 218 | The role of promoters for Ni catalysts in low temperature (membrane) steam methane reforming. Applied Catalysis A: General, 2011, 405, 108-119. | 4.3 | 49 |
| 219 | On the structure and hydrotreating performance of carbon-supported CoMo- and NiMo-sulfides. Applied Catalysis B: Environmental, 2013, 142-143, 178-186. | 20.2 | 49 |
| 220 | Molecular Promoting of Aluminum Metal–Organic Framework Topology MIL-101 by <i>N</i> , <i>N</i> -Dimethylformamide. Inorganic Chemistry, 2014, 53, 882-887. | 4.0 | 49 |
| 221 | Hydride Transfer versus Deprotonation Kinetics in the Isobutane–Propene Alkylation Reaction: A Computational Study. ACS Catalysis, 2017, 7, 8613-8627. | 11.2 | 49 |
| 222 | Size and Topological Effects of Rhodium Surfaces, Clusters and Nanoparticles on the Dissociation of CO. Journal of Physical Chemistry C, 2011, 115, 14204-14212. | 3.1 | 48 |
| 223 | Unprecedented Oxygenate Selectivity in Aqueousâ€Phase Fischer–Tropsch Synthesis by Ruthenium Nanoparticles. ChemCatChem, 2011, 3, 1735-1738. | 3.7 | 48 |
| 224 | Synthesis of hierarchical zeolites using an inexpensive mono-quaternary ammonium surfactant as mesoporogen. Chemical Communications, 2014, 50, 14658-14661. | 4.1 | 48 |
| 225 | Density Functional Theory Study of the Mechanism of Formaldehyde Oxidation on Mn-Doped Ceria. Journal of Physical Chemistry C, 2016, 120, 13071-13077. | 3.1 | 48 |
| 226 | Efficient Conversion of Pine Wood Lignin to Phenol. ChemSusChem, 2020, 13, 1705-1709. | 6.8 | 48 |
| 227 | The Molecular Pathway to ZIFâ€7 Microrods Revealed by In Situ Timeâ€Resolved Small―and Wideâ€Angle Xâ€R Scattering, Quickâ€5canning Extended Xâ€Ray Absorption Spectroscopy, and DFT Calculations. Chemistry - A European Journal, 2013, 19, 7809-7816. | ay 3.3 | 47 |
| 228 | Relevance of the Mo-precursor state in H-ZSM-5 for methane dehydroaromatization. Catalysis Science and Technology, 2018, 8, 916-922. | 4.1 | 47 |
| 229 | The effect of oxidation and resulfidation on (Ni/Co)MoS2 hydrodesulfurisation catalysts. Applied Catalysis B: Environmental, 2019, 243, 145-150. | 20.2 | 47 |
| 230 | Surface functionalization of SBA-15-ordered mesoporous silicas: Oxidation of benzene to phenol by nitrous oxide. Journal of Catalysis, 2008, 255, 190-196. | 6.2 | 46 |
| 231 | Au/TiO2@SBA-15 nanocomposites as catalysts for direct propylene epoxidation with O2 and H2 mixtures. Journal of Catalysis, 2011, 282, 94-102. | 6.2 | 46 |
| 232 | Silylation enhances the performance of Au/Ti–SiO2 catalysts in direct epoxidation of propene using H2 and O2. Journal of Catalysis, 2016, 344, 434-444. | 6.2 | 46 |
| 233 | Effect of proximity and support material on deactivation of bifunctional catalysts for the conversion of synthesis gas to olefins and aromatics. Catalysis Today, 2020, 342, 161-166. | 4.4 | 46 |
| 234 | Low-Temperature Ammonia Oxidation Over Pt/γ-Alumina: The Influence of the Alumina Support. Topics in Catalysis, 2003, 23, 109-117. | 2.8 | 45 |

| # | Article | IF | CITATIONS |
|-----|--|-----------------|---------------------|
| 235 | Structure Sensitivity in CO Oxidation by a Single Au Atom Supported on Ceria. Journal of Physical Chemistry C, 2013, 117, 7721-7726. | 3.1 | 45 |
| 236 | A Periodic DFT Study of Glucose to Fructose Isomerization on Tungstite (WO ₃ A·H ₂ O): Influence of Group IV–VI Dopants and Cooperativity with Hydroxyl Groups. ACS Catalysis, 2016, 6, 4162-4169. | 11.2 | 45 |
| 237 | Optimum Particle Size for Gold-Catalyzed CO Oxidation. Journal of Physical Chemistry C, 2018, 122, 8327-8340. | 3.1 | 45 |
| 238 | Unraveling the Role of Lithium in Enhancing the Hydrogen Evolution Activity of MoS ₂ : Intercalation versus Adsorption. ACS Energy Letters, 2019, 4, 1733-1740. | 17.4 | 45 |
| 239 | In situ X-ray absorption spectroscopy of germanium evaporated thin film electrodes. Electrochimica Acta, 2010, 55, 7074-7079. | 5.2 | 44 |
| 240 | Carbon-Induced Surface Transformations of Cobalt. ACS Catalysis, 2015, 5, 596-601. | 11.2 | 44 |
| 241 | Identifying Sn Site Heterogeneities Prevalent Among Snâ€Beta Zeolites. Helvetica Chimica Acta, 2016, 99, 916-927. | 1.6 | 44 |
| 242 | On the Role of Acidity in Bulk and Nanosheet [T]MFI (T=Al ³⁺ _, Ga ³⁺ ,) Tj E 2017, 9, 3942-3954. | TQq0 0 0 3.7 | rgBT /Overloc 44 |
| 243 | Stability of heterogeneous single-atom catalysts: a scaling law mapping thermodynamics to kinetics. Npj Computational Materials, 2020, 6, . | 8.7 | 44 |
| 244 | Improved Pd/CeO ₂ Catalysts for Low-Temperature NO Reduction: Activation of CeO ₂ Lattice Oxygen by Fe Doping. ACS Catalysis, 2021, 11, 5614-5627. | 11.2 | 44 |
| 245 | CO–PROX reactions on copper cerium oxide catalysts prepared by melt infiltration. Applied Catalysis B: Environmental, 2012, 123-124, 424-432. | 20.2 | 43 |
| 246 | Catalytic properties of extraframework iron-containing species in ZSM-5 for N2O decomposition. Journal of Catalysis, 2013, 308, 386-397. | 6.2 | 43 |
| 247 | Microkinetics of steam methane reforming on platinum and rhodium metal surfaces. Journal of Catalysis, 2013, 297, 227-235. | 6.2 | 43 |
| 248 | Photocatalytic decarboxylation of lactic acid by Pt/TiO ₂ . Chemical Communications, 2016, 52, 11634-11637. | 4.1 | 43 |
| 249 | Hierarchical 2D yarn-ball like metal–organic framework NiFe(dobpdc) as bifunctional electrocatalyst for efficient overall electrocatalytic water splitting. Journal of Materials Chemistry A, 2020, 8, 22974-22982. | 10.3 | 43 |
| 250 | Different mechanisms of ethane aromatization over Mo/ZSM-5 and Ga/ZSM-5 catalysts. Catalysis Today, 2021, 369, 184-192. | 4.4 | 43 |
| 251 | Site regeneration in the Fischer–Tropsch synthesis reaction: a synchronized CO dissociation and C–C coupling pathway. Chemical Communications, 2011, 47, 9822. | 4.1 | 42 |
| 252 | Reactivity of CO on Carbon-Covered Cobalt Surfaces in Fischer–Tropsch Synthesis. Journal of Physical Chemistry C, 2014, 118, 5317-5327. | 3.1 | 42 |

| # | Article | IF | CITATIONS |
|-----|--|------|-----------|
| 253 | Supported nickel–rhenium catalysts for selective hydrogenation of methyl esters to alcohols. Chemical Communications, 2017, 53, 9761-9764. | 4.1 | 42 |
| 254 | Reversible Restructuring of Silver Particles during Ethylene Epoxidation. ACS Catalysis, 2018, 8, 11794-11800. | 11.2 | 42 |
| 255 | Catalytic conversion of furanic compounds over Ga-modified ZSM-5 zeolites as a route to biomass-derived aromatics. Green Chemistry, 2018, 20, 3818-3827. | 9.0 | 42 |
| 256 | Highly efficient CO ₂ electrolysis within a wide operation window using octahedral tin oxide single crystals. Journal of Materials Chemistry A, 2021, 9, 7848-7856. | 10.3 | 42 |
| 257 | Influence of support morphology on the detemplation and permeation of ZSM-5 and SSZ-13 zeolite membranes. Microporous and Mesoporous Materials, 2014, 197, 268-277. | 4.4 | 41 |
| 258 | Hydrogenation of Î ³ -valerolactone in ethanol over Pd nanoparticles supported on sulfonic acid functionalized MIL-101. RSC Advances, 2014, 4, 39558. | 3.6 | 41 |
| 259 | Stable Surface-Anchored Cu Nanocubes for CO ₂ Electroreduction to Ethylene. ACS Applied Nano Materials, 2020, 3, 8328-8334. | 5.0 | 41 |
| 260 | Lignin-Based Additives for Improved Thermo-Oxidative Stability of Biolubricants. ACS Sustainable Chemistry and Engineering, 2021, 9, 12548-12559. | 6.7 | 41 |
| 261 | Encapsulation of transition metal sulfides in faujasite zeolite for hydroprocessing applications. Catalysis Today, 2003, 86, 87-109. | 4.4 | 40 |
| 262 | Intrinsic kinetics of thiophene hydrodesulfurization on a sulfided NiMo/SiO2 planar model catalyst. Journal of Catalysis, 2004, 221, 541-548. | 6.2 | 40 |
| 263 | Correlating Fischer–Tropsch activity to Ru nanoparticle surface structure as probed by high-energy X-ray diffraction. Chemical Communications, 2014, 50, 6005-6008. | 4.1 | 40 |
| 264 | Selective Propylene Oxidation to Acrolein by Gold Dispersed on MgCuCr ₂ O ₄ Spinel. ACS Catalysis, 2015, 5, 1100-1111. | 11.2 | 40 |
| 265 | Influence of Pt particle size and Re addition by catalytic reduction on aqueous phase reforming of glycerol for carbon-supported Pt(Re) catalysts. Applied Catalysis B: Environmental, 2015, 174-175, 126-135. | 20.2 | 40 |
| 266 | Nonâ€Pincerâ€Type Manganese Complexes as Efficient Catalysts for the Hydrogenation of Esters. Angewandte Chemie, 2017, 129, 7639-7642. | 2.0 | 40 |
| 267 | Influence of pore topology on synthesis and reactivity of Sn-modified zeolite catalysts for carbohydrate conversions. Catalysis Science and Technology, 2017, 7, 3151-3162. | 4.1 | 40 |
| 268 | A site-sensitive quasi-in situ strategy to characterize Mo/HZSM-5 during activation. Journal of Catalysis, 2019, 370, 321-331. | 6.2 | 40 |
| 269 | Mechanistic role of protonated polar additives in ethanol for selective transformation of biomass-related compounds. Applied Catalysis B: Environmental, 2020, 264, 118509. | 20.2 | 40 |
| 270 | The influence of metal loading and activation on mesoporous materials supported nickel phosphide hydrotreating catalysts. Applied Catalysis A: General, 2009, 365, 48-54. | 4.3 | 39 |

| # | Article | IF | CITATIONS |
|-----|---|------|-----------|
| 271 | Acidic properties of nanolayered ZSM-5 zeolites. Microporous and Mesoporous Materials, 2014, 189, 144-157. | 4.4 | 39 |
| 272 | On the metal–support synergy for selective gas-phase ethanol oxidation over MgCuCr 2 O 4 supported metal nanoparticle catalysts. Journal of Catalysis, 2015, 331, 138-146. | 6.2 | 39 |
| 273 | A real support effect on the hydrodeoxygenation of methyl oleate by sulfided NiMo catalysts. Catalysis Today, 2017, 298, 181-189. | 4.4 | 39 |
| 274 | Mechanism of Carbon Monoxide Dissociation on a Cobalt Fischer–Tropsch Catalyst. ChemCatChem, 2018, 10, 136-140. | 3.7 | 39 |
| 275 | Electronic Structure and Interface Energetics of CuBi ₂ O ₄ Photoelectrodes. Journal of Physical Chemistry C, 2020, 124, 22416-22425. | 3.1 | 39 |
| 276 | Activation of Mo/HZSM-5 for methane aromatization. Chinese Journal of Catalysis, 2015, 36, 829-837. | 14.0 | 38 |
| 277 | Tracking Local Mechanical Impact in Heterogeneous Polymers with Direct Optical Imaging. Angewandte Chemie - International Edition, 2018, 57, 16385-16390. | 13.8 | 38 |
| 278 | Structure sensitivity in the hydrogenation of unsaturated hydrocarbons over Rh nanoparticles. Catalysis Today, 2012, 183, 72-78. | 4.4 | 37 |
| 279 | A computational study of the influence of the ceria surface termination on the mechanism of CO oxidation of isolated Rh atoms. Faraday Discussions, 2013, 162, 281. | 3.2 | 37 |
| 280 | Coverage Effects in CO Dissociation on Metallic Cobalt Nanoparticles. ACS Catalysis, 2019, 9, 7365-7372. | 11.2 | 37 |
| 281 | Water-Dispersible Copper Sulfide Nanocrystals via Ligand Exchange of 1-Dodecanethiol. Chemistry of Materials, 2019, 31, 541-552. | 6.7 | 37 |
| 282 | The Vital Role of Step-Edge Sites for Both CO Activation and Chain Growth on Cobalt Fischer–Tropsch Catalysts Revealed through First-Principles-Based Microkinetic Modeling Including Lateral Interactions. ACS Catalysis, 2020, 10, 9376-9400. | 11.2 | 37 |
| 283 | Cyanide leaching of Au/CeO2: highly active gold clusters for 1,3-butadiene hydrogenation. Physical Chemistry Chemical Physics, 2009, 11, 9578-82. | 2.8 | 36 |
| 284 | Site Stability on Cobalt Nanoparticles: A Molecular Dynamics ReaxFF Reactive Force Field Study. Journal of Physical Chemistry C, 2014, 118, 6882-6886. | 3.1 | 36 |
| 285 | Texture, acidity and fluid catalytic cracking performance of hierarchical faujasite zeolite prepared by an amphiphilic organosilane. Fuel Processing Technology, 2015, 139, 248-258. | 7.2 | 36 |
| 286 | Competitive Adsorption of Substrate and Solvent in Snâ€Beta Zeolite During Sugar Isomerization. ChemSusChem, 2016, 9, 3145-3149. | 6.8 | 36 |
| 287 | Transition metal (Ti, Mo, Nb, W) nitride catalysts for lignin depolymerisation. Chemical Communications, 2016, 52, 9375-9378. | 4.1 | 36 |
| 288 | Fluoride-assisted synthesis of bimodal microporous SSZ-13 zeolite. Chemical Communications, 2016, 52, 3227-3230. | 4.1 | 36 |

| # | Article | IF | CITATIONS |
|-----|---|------|-----------|
| 289 | One-pot synthesis of nano-crystalline MCM-22. Microporous and Mesoporous Materials, 2016, 220, 28-38. | 4.4 | 36 |
| 290 | Synergy in Lignin Upgrading by a Combination of Cu-Based Mixed Oxide and Ni-Phosphide Catalysts in Supercritical Ethanol. ACS Sustainable Chemistry and Engineering, 2017, 5, 3535-3543. | 6.7 | 36 |
| 291 | Understanding the Impact of Defects on Catalytic CO Oxidation of LaFeO ₃ -Supported Rh, Pd, and Pt Single-Atom Catalysts. Journal of Physical Chemistry C, 2019, 123, 7290-7298. | 3.1 | 36 |
| 292 | Insight into the Rate-Determining Step and Active Sites in the Fischer–Tropsch Reaction over Cobalt Catalysts. ACS Catalysis, 2019, 9, 4189-4195. | 11.2 | 36 |
| 293 | Kinetic model for adsorption and desorption of H2O and CO2 on hydrotalcite-based adsorbents. Chemical Engineering Journal, 2019, 355, 520-531. | 12.7 | 36 |
| 294 | On the sulfur tolerance of supported Ni(Co)Mo sulfide hydrotreating catalysts. Journal of Catalysis, 2003, 215, 353-357. | 6.2 | 35 |
| 295 | Methane Dissociation on High and Low Indices Rh Surfaces. Journal of Physical Chemistry C, 2011, 115, 13027-13034. | 3.1 | 35 |
| 296 | The Optimally Performing Fischer–Tropsch Catalyst. Angewandte Chemie, 2014, 126, 12960-12964. | 2.0 | 35 |
| 297 | Stability of CoP _{<i>x</i>} Electrocatalysts in Continuous and Interrupted Acidic Electrolysis of Water. ChemElectroChem, 2018, 5, 1230-1239. | 3.4 | 35 |
| 298 | Investigation of the stability of NiFe-(oxy)hydroxide anodes in alkaline water electrolysis under industrially relevant conditions. Catalysis Science and Technology, 2020, 10, 5593-5601. | 4.1 | 35 |
| 299 | Catalytic Hydrogenation of Renewable Levulinic Acid to Î ³ -Valerolactone: Insights into the Influence of Feed Impurities on Catalyst Performance in Batch and Flow Reactors. ACS Sustainable Chemistry and Engineering, 2020, 8, 5903-5919. | 6.7 | 35 |
| 300 | Characterization and thiophene hydrodesulfurization activity of amorphous-silica–alumina-supported NiW catalysts. Journal of Catalysis, 2004, 228, 433-446. | 6.2 | 34 |
| 301 | Non-localized charge compensation in zeolites: A periodic DFT study of cationic gallium-oxide clusters in mordenite. Journal of Catalysis, 2008, 255, 139-143. | 6.2 | 34 |
| 302 | Template-Free Synthesis of Sphere, Rod and Prism Morphologies of CeO2 Oxidation Catalysts. Catalysis Letters, 2010, 137, 28-34. | 2.6 | 34 |
| 303 | Palladium nanoparticles entrapped in polymeric ionic liquid microgels as recyclable hydrogenation catalysts. Journal of Molecular Catalysis A, 2013, 379, 53-58. | 4.8 | 34 |
| 304 | Multiple Zeolite Structures from One Ionic Liquid Template. Chemistry - A European Journal, 2013, 19, 2122-2130. | 3.3 | 34 |
| 305 | Acid catalytic properties of reduced tungsten and niobium-tungsten oxides. Applied Catalysis B: Environmental, 2015, 163, 370-381. | 20.2 | 34 |
| 306 | Looking at the Future of Chemical Production through the European Roadmap on Science and Technology of Catalysis the EU Effort for a Longâ€ŧerm Vision. ChemCatChem, 2017, 9, 904-909. | 3.7 | 34 |

| # | Article | IF | CITATIONS |
|-----|---|------|-----------|
| 307 | Continuous Synthesis of γ-Valerolactone in a Trickle-Bed Reactor over Supported Nickel Catalysts. Industrial & Engineering Chemistry Research, 2017, 56, 2680-2689. | 3.7 | 34 |
| 308 | Direct synthesis of hierarchical ZSM-5 zeolite using cetyltrimethylammonium as structure directing agent for methanol-to-hydrocarbons conversion. Catalysis Science and Technology, 2017, 7, 4520-4533. | 4.1 | 34 |
| 309 | Quantum-Chemical DFT Study of Direct and H- and C-Assisted CO Dissociation on the χ-Fe ₅ C ₂ HÃǥg Carbide. Journal of Physical Chemistry C, 2018, 122, 9929-9938. | 3.1 | 34 |
| 310 | Aerobic Oxidation of 5â€(Hydroxymethyl)furfural Cyclic Acetal Enables Selective Furanâ€2,5â€dicarboxylic Acid Formation with CeO ₂ â€Supported Gold Catalyst. Angewandte Chemie, 2018, 130, 8367-8371. | 2.0 | 34 |
| 311 | Transition metal doping of Pd(1 1 1) for the NO + CO reaction. Journal of Catalysis, 2018, 363, 154-163. | 6.2 | 34 |
| 312 | Structure Sensitivity of Silver-Catalyzed Ethylene Epoxidation. ACS Catalysis, 2019, 9, 9829-9839. | 11.2 | 34 |
| 313 | Supported Pt-Re catalysts for the selective hydrogenation of methyl and ethyl esters to alcohols. Catalysis Today, 2017, 279, 10-18. | 4.4 | 33 |
| 314 | High-pressure sulfidation of a calcined CoMo/Al2O3 hydrodesulfurization catalyst. Catalysis Today, 2008, 130, 126-134. | 4.4 | 32 |
| 315 | DFT Simulations of Water Adsorption and Activation on Lowâ€Index αâ€Ga ₂ O ₃ Surfaces. Chemistry - A European Journal, 2014, 20, 6915-6926. | 3.3 | 32 |
| 316 | Photoelectrochemical Properties of CuCrO2: Characterization of Light Absorption and Photocatalytic H2 Production Performance. Catalysis Letters, 2014, 144, 1487-1493. | 2.6 | 32 |
| 317 | Mesoporous Doped Tungsten Oxide for Glucose Dehydration to 5-Hydroxymethylfurfural. ACS Sustainable Chemistry and Engineering, 2019, 7, 7552-7562. | 6.7 | 32 |
| 318 | On the Stability of Co ₃ O ₄ Oxygen Evolution Electrocatalysts in Acid. ChemCatChem, 2021, 13, 459-467. | 3.7 | 32 |
| 319 | Quasi in Situ Sequential Sulfidation of CoMo/Al2O3Studied Using High-Resolution Electron Microscopy. Journal of Physical Chemistry B, 2002, 106, 11795-11799. | 2.6 | 31 |
| 320 | Activation of ammonia dissociation by oxygen on platinum sponge studied with positron emission profiling. Journal of Catalysis, 2003, 219, 156-166. | 6.2 | 31 |
| 321 | DFT study on H2O activation by stepped and planar Rh surfaces. Surface Science, 2009, 603, 3275-3281. | 1.9 | 31 |
| 322 | Improving separation performance of high-silica zeolite membranes by surface modification with triethoxyfluorosilane. Microporous and Mesoporous Materials, 2014, 194, 24-30. | 4.4 | 31 |
| 323 | Stability and catalytic properties of porous acidic (organo)silica materials for conversion of carbohydrates. Journal of Molecular Catalysis A, 2014, 388-389, 81-89. | 4.8 | 31 |
| 324 | Deactivation of Sn-Beta during carbohydrate conversion. Applied Catalysis A: General, 2018, 564, 113-122. | 4.3 | 31 |

| # | Article | IF | CITATIONS |
|-----|--|------|-----------|
| 325 | Tunable colloidal Ni nanoparticles confined and redistributed in mesoporous silica for CO ₂ methanation. Catalysis Science and Technology, 2019, 9, 2578-2591. | 4.1 | 31 |
| 326 | Lattice oxygen activation in transition metal doped ceria. Chinese Journal of Catalysis, 2020, 41, 977-984. | 14.0 | 31 |
| 327 | Effect of the Nature and Location of Copper Species on the Catalytic Nitric Oxide Selective Catalytic Reduction Performance of the Copper/SSZâ€13 Zeolite. ChemCatChem, 2014, 6, 634-639. | 3.7 | 30 |
| 328 | Silica-supported Ni 2 P: Effect of preparation conditions on structure and catalytic performance in thiophene hydrodesulfurization (HDS). Catalysis Today, 2017, 292, 121-132. | 4.4 | 30 |
| 329 | Ceria–zirconia encapsulated Ni nanoparticles for CO ₂ methanation. Catalysis Science and Technology, 2019, 9, 5001-5010. | 4.1 | 30 |
| 330 | Electrochemical stability of RuO2(110)/Ru(0001) model electrodes in the oxygen and chlorine evolution reactions. Electrochimica Acta, 2020, 336, 135713. | 5.2 | 30 |
| 331 | Iron-functionalized Al-SBA-15 for benzene hydroxylation. Chemical Communications, 2008, , 774-776. | 4.1 | 29 |
| 332 | The CO Formation Reaction Pathway in Steam Methane Reforming by Rhodium. Langmuir, 2010, 26, 16339-16348. | 3.5 | 29 |
| 333 | Co-Aromatization of Furan and Methanol over ZSM-5—A Pathway to Bio-Aromatics. ACS Catalysis, 2019, 9, 8547-8554. | 11.2 | 29 |
| 334 | First-principles based microkinetic modeling of transient kinetics of CO hydrogenation on cobalt catalysts. Catalysis Today, 2020, 342, 131-141. | 4.4 | 29 |
| 335 | On the surface-dependent oxidation of Cu2O during CO oxidation: Cu2+ is more active than Cu+. Applied Catalysis A: General, 2020, 602, 117712. | 4.3 | 29 |
| 336 | Stabilization effects in binary colloidal Cu and Ag nanoparticle electrodes under electrochemical CO ₂ reduction conditions. Nanoscale, 2021, 13, 4835-4844. | 5.6 | 29 |
| 337 | The observation of nanometer-sized entities in sulphided Mo-based catalysts on various supports. Catalysis Letters, 2001, 74, 49-53. | 2.6 | 28 |
| 338 | Controlling Reaction Pathways for Alcohol Dehydration and Dehydrogenation over FeSBA-15 Catalysts. Catalysis Letters, 2007, 117, 18-24. | 2.6 | 28 |
| 339 | How metallic is gold in the direct epoxidation of propene: an FTIR study. Catalysis Science and Technology, 2013, 3, 3042. | 4.1 | 28 |
| 340 | Furfural hydrodeoxygenation (HDO) over silica-supported metal phosphides – The influence of metal–phosphorus stoichiometry on catalytic properties. Journal of Catalysis, 2021, 403, 181-193. | 6.2 | 28 |
| 341 | Nature of Enhanced BrÃ,nsted Acidity Induced by Extraframework Aluminum in an Ultrastabilized Faujasite Zeolite: An <i>In Situ</i> NMR Study. Journal of Physical Chemistry C, 2021, 125, 9050-9059. | 3.1 | 28 |
| 342 | Formation of a Rhodium Surface Oxide Film in Rh _{<i>n</i>} /CeO ₂ (111) Relevant for Catalytic CO Oxidation: A Computational Study. Journal of Physical Chemistry C, 2012, 116, 22904-22915. | 3.1 | 27 |

| # | Article | IF | CITATIONS |
|-----|--|------|-----------|
| 343 | Tuning the hydrogenation activity of Pd NPs on Al–MIL-53 by linker modification. Catalysis Science and Technology, 2014, 4, 795. | 4.1 | 27 |
| 344 | Optimization of Au0–Cu+ synergy in Au/MgCuCr2O4 catalysts for aerobic oxidation of ethanol to acetaldehyde. Journal of Catalysis, 2017, 347, 45-56. | 6.2 | 27 |
| 345 | A Density Functional Theory Study of the Mechanism of Direct Glucose Dehydration to 5â€Hydroxymethylfurfural on Anatase Titania. ChemCatChem, 2018, 10, 4084-4089. | 3.7 | 27 |
| 346 | Finite-Temperature Structures of Supported Subnanometer Catalysts Inferred <i>via</i> Statistical Learning and Genetic Algorithm-Based Optimization. ACS Nano, 2020, 14, 13995-14007. | 14.6 | 27 |
| 347 | Tuning the reactivity of molybdenum (oxy)carbide catalysts by the carburization degree: CO ₂ reduction and anisole hydrodeoxygenation. Catalysis Science and Technology, 2020, 10, 3635-3645. | 4.1 | 27 |
| 348 | Impact of small promoter amounts on coke structure in dry reforming of methane over Ni/ZrO ₂ . Catalysis Science and Technology, 2020, 10, 3965-3974. | 4.1 | 27 |
| 349 | Anionic Oligomerization of Ethylene over Ga/ZSM-5 Zeolite: A Theoretical Study. Journal of Physical Chemistry C, 2008, 112, 19604-19611. | 3.1 | 26 |
| 350 | Detection of Carbocationic Species in Zeolites: Large Crystals Pave the Way. Chemistry - A European Journal, 2010, 16, 9340-9348. | 3.3 | 26 |
| 351 | On the effect of EDTA treatment on the acidic properties of USY zeolite and its performance in vacuum gas oil hydrocracking. Applied Catalysis A: General, 2014, 488, 219-230. | 4.3 | 26 |
| 352 | Structure sensitivity in the ruthenium nanoparticle catalyzed aqueous-phase Fischer–Tropsch reaction. Catalysis Science and Technology, 2014, 4, 3510-3523. | 4.1 | 26 |
| 353 | Influence of material composition on the CO2 and H2O adsorption capacities and kinetics of potassium-promoted sorbents. Chemical Engineering Journal, 2018, 334, 2115-2123. | 12.7 | 26 |
| 354 | A Facile Direct Route to <i>N</i> â€{Un)substituted Lactams by Cycloamination of Oxocarboxylic Acids without External Hydrogen. ChemSusChem, 2019, 12, 3778-3784. | 6.8 | 26 |
| 355 | Enumerating Active Sites on Metal Nanoparticles: Understanding the Size Dependence of Cobalt Particles for CO Dissociation. ACS Catalysis, 2021, 11, 8484-8492. | 11.2 | 26 |
| 356 | Layered double hydroxides as catalysts for aromatic nitrile hydrolysis. Microporous and Mesoporous Materials, 2002, 56, 241-255. | 4.4 | 25 |
| 357 | A theoretical study of the reverse waterâ€gas shift reaction on Ni(111) and Ni(311) surfaces. Canadian Journal of Chemical Engineering, 2020, 98, 740-748. | 1.7 | 25 |
| 358 | Investigation of the Active Phase in K-Promoted MoS ₂ Catalysts for Methanethiol Synthesis. ACS Catalysis, 2020, 10, 1838-1846. | 11.2 | 25 |
| 359 | Reactivity of generated oxygen species from nitrous oxide over [Fe,Al]MFI catalysts for the direct oxidation of benzene to phenol. Catalysis Today, 2005, 110, 221-227. | 4.4 | 24 |
| 360 | Influence of chloride ions on the stability of PtNi alloys for PEMFC cathode. Electrochimica Acta, 2011, 56, 7235-7242. | 5.2 | 24 |

| # | Article | IF | CITATIONS |
|-----|---|------|-----------|
| 361 | Synthesis and separation properties of an α-alumina-supported high-silica MEL membrane. Journal of Membrane Science, 2013, 447, 12-18. | 8.2 | 24 |
| 362 | Reconstruction of Clean and Oxygen-Covered Pt(110) Surfaces. Journal of Physical Chemistry C, 2013, 117, 11251-11257. | 3.1 | 24 |
| 363 | Nitrogen-doping of bulk and nanotubular TiO2 photocatalysts by plasma-assisted atomic layer deposition. Applied Surface Science, 2015, 330, 476-486. | 6.1 | 24 |
| 364 | Decomposition of lignin model compounds by Lewis acid catalysts in water and ethanol. Journal of Molecular Catalysis A, 2015, 410, 89-99. | 4.8 | 24 |
| 365 | Role of Dissociatively Adsorbed Water on the Formation of Shallow Trapped Electrons in TiO ₂ Photocatalysts. Journal of Physical Chemistry C, 2017, 121, 10153-10162. | 3.1 | 24 |
| 366 | Mechanistic aspects of n-paraffins hydrocracking: Influence of zeolite morphology and acidity of Pd(Pt)/ZSM-5 catalysts. Journal of Catalysis, 2020, 389, 544-555. | 6.2 | 24 |
| 367 | Dry gel conversion of organosilane templated mesoporous silica: from amorphous to crystalline catalysts for benzene oxidation. Journal of Materials Chemistry, 2011, 21, 9279. | 6.7 | 23 |
| 368 | The relative stability of zeolite precursor tetraalkylammonium–silicate oligomer complexes. Microporous and Mesoporous Materials, 2011, 146, 82-87. | 4.4 | 23 |
| 369 | A Mechanistic Study of Niâ€catalyzed Carbon Dioxide Coupling with Ethylene towards the Manufacture of Acrylic Acid. ChemCatChem, 2014, 6, 800-807. | 3.7 | 23 |
| 370 | A mechanism of gas-phase alcohol oxidation at the interface of Au nanoparticles and a MgCuCr ₂ O ₄ spinel support. Catalysis Science and Technology, 2014, 4, 2997-3003. | 4.1 | 23 |
| 371 | Development of a heterogeneous catalyst for lignocellulosic biomass conversion: Glucose dehydration by metal chlorides in a silicaâ€supported ionic liquid layer. Environmental Progress and Sustainable Energy, 2014, 33, 657-662. | 2.3 | 23 |
| 372 | Bent Carbon Surface Moieties as Active Sites on Carbon Catalysts for Phosgene Synthesis. Angewandte Chemie - International Edition, 2016, 55, 1728-1732. | 13.8 | 23 |
| 373 | Electronic Structure Analysis of the Diels–Alder Cycloaddition Catalyzed by Alkali-Exchanged Faujasites. Journal of Physical Chemistry C, 2018, 122, 14733-14743. | 3.1 | 23 |
| 374 | Industrial lignin from 2G biorefineries – Assessment of availability and pricing strategies. Bioresource Technology, 2019, 291, 121805. | 9.6 | 23 |
| 375 | Influence of Reduced Cu Surface States on the Photoelectrochemical Properties of CuBi ₂ O ₄ . ACS Applied Energy Materials, 2019, 2, 6866-6874. | 5.1 | 23 |
| 376 | Towards a quantitative determination of strain in Bragg Coherent X-ray Diffraction Imaging: artefacts and sign convention in reconstructions. Scientific Reports, 2019, 9, 17357. | 3.3 | 23 |
| 377 | Mechanistic Insight into the [4 + 2] Diels–Alder Cycloaddition over First Row d-Block Cation-Exchanged Faujasites. ACS Catalysis, 2019, 9, 376-391. | 11.2 | 23 |
| 378 | Spin design of iron complexes on Fe-ZSM-5 zeolites. Catalysis Today, 2005, 110, 247-254. | 4.4 | 22 |

| # | Article | IF | CITATIONS |
|-----|--|------|-----------|
| 379 | The nature of the sulfur tolerance of amorphous silica-alumina supported NiMo(W) sulfide and Pt hydrogenation catalysts. Applied Catalysis A: General, 2012, 411-412, 51-59. | 4.3 | 22 |
| 380 | Chemical Vapor Deposition of Trimethylaluminum on Dealuminated Faujasite Zeolite. ACS Catalysis, 2013, 3, 1504-1517. | 11.2 | 22 |
| 381 | Platinum–Rhenium Synergy on Reducible Oxide Supports in Aqueousâ€Phase Glycerol Reforming. ChemCatChem, 2014, 6, 1260-1269. | 3.7 | 22 |
| 382 | Cellulose conversion to ethylene glycol by tungsten oxide-based catalysts. Molecular Catalysis, 2019, 473, 110400. | 2.0 | 22 |
| 383 | Hierarchically porous FER zeolite obtained via FAU transformation for fatty acid isomerization. Applied Catalysis B: Environmental, 2020, 263, 118356. | 20.2 | 22 |
| 384 | Physicochemical and catalytic characterization of non-hydrothermally synthesized Mg-, Ni- and Mg–Ni-saponite-like materials. Microporous and Mesoporous Materials, 2004, 69, 49-63. | 4.4 | 21 |
| 385 | Roughening of Pt nanoparticles induced by surface-oxide formation. Physical Chemistry Chemical Physics, 2013, 15, 2268. | 2.8 | 21 |
| 386 | Establishing hierarchy: the chain of events leading to the formation of silicalite-1 nanosheets. Chemical Science, 2016, 7, 6506-6513. | 7.4 | 21 |
| 387 | Multiâ€site Cooperativity in Alkaliâ€Metalâ€Exchanged Faujasites for the Production of Biomassâ€Derived Aromatics. ChemPhysChem, 2018, 19, 446-458. | 2.1 | 21 |
| 388 | Mild thermolytic solvolysis of technical lignins in polar organic solvents to a crude lignin oil. Sustainable Energy and Fuels, 2020, 4, 6212-6226. | 4.9 | 21 |
| 389 | <i>Inâ€Situ</i> Shellâ€Isolated Nanoparticleâ€Enhanced Raman Spectroscopy of Nickelâ€Catalyzed Hydrogenation Reactions. ChemPhysChem, 2020, 21, 625-632. | 2.1 | 21 |
| 390 | Dynamics of silver particles during ethylene epoxidation. Applied Catalysis B: Environmental, 2020, 272, 118983. | 20.2 | 21 |
| 391 | Promoting oxygen evolution of IrO2 in acid electrolyte by Mn. Electrochimica Acta, 2021, 366, 137448. | 5.2 | 21 |
| 392 | Selective hydrogen oxidation in a mixture with ethane/ethene using cerium zirconium oxide. Applied Catalysis A: General, 2004, 262, 201-206. | 4.3 | 20 |
| 393 | Preparation and photoelectrochemical properties of nitrogen doped nanotubular TiO2 arrays. Applied Surface Science, 2013, 282, 174-180. | 6.1 | 20 |
| 394 | A Robust Au/ZnCr ₂ O ₄ Catalyst with Highly Dispersed Gold Nanoparticles for Gas-Phase Selective Oxidation of Cyclohexanol to Cyclohexanone. ACS Catalysis, 2019, 9, 11104-11115. | 11.2 | 20 |
| 395 | Dynamics of gold clusters on ceria during CO oxidation. Journal of Catalysis, 2020, 392, 39-47. | 6.2 | 20 |
| 396 | Effect of Organic Capping Agents on Rutheniumâ€Nanoparticleâ€Catalyzed Aqueousâ€Phase Fischer–Tropsch Synthesis. ChemCatChem, 2013, 5, 3148-3155. | 3.7 | 19 |

| # | Article | IF | CITATIONS |
|-----|--|------|-----------|
| 397 | Probing the Influence of SSZâ€13 Zeolite Pore Hierarchy in Methanolâ€toâ€Olefins Catalysis by Using Nanometer Accuracy by Stochastic Chemical Reactions Fluorescence Microscopy and Positron Emission Profiling. ChemCatChem, 2017, 9, 3470-3477. | 3.7 | 19 |
| 398 | Bio-Based Chemicals: Selective Aerobic Oxidation of Tetrahydrofuran-2,5-dimethanol to Tetrahydrofuran-2,5-dicarboxylic Acid Using Hydrotalcite-Supported Gold Catalysts. ACS Sustainable Chemistry and Engineering, 2019, 7, 4647-4656. | 6.7 | 19 |
| 399 | Interfacial charge transfer in Pt-loaded TiO2 P25 photocatalysts studied by in-situ diffuse reflectance FTIR spectroscopy of adsorbed CO. Journal of Photochemistry and Photobiology A: Chemistry, 2019, 370, 84-88. | 3.9 | 19 |
| 400 | Evidence of Octahedral Co–Mo–S Sites in Hydrodesulfurization Catalysts as Determined by Resonant Inelastic X-ray Scattering and X-ray Absorption Spectroscopy. ACS Catalysis, 2020, 10, 10978-10988. | 11.2 | 19 |
| 401 | Direct Hydrothermal Synthesis of Iron-Containing Mesoporous Silica SBA-15: Potential as a Support for Gold Nanoparticles. Journal of Physical Chemistry C, 2009, 113, 21831-21839. | 3.1 | 18 |
| 402 | Hydrothermal synthesis and characterization of a layered zirconium silicate. Microporous and Mesoporous Materials, 2013, 180, 48-55. | 4.4 | 18 |
| 403 | Selective Coke Combustion by Oxygen Pulsing During Mo/ZSMâ€5â€Catalyzed Methane Dehydroaromatization. Angewandte Chemie, 2016, 128, 15310-15314. | 2.0 | 18 |
| 404 | Identification of step-edge sites on Rh nanoparticles for facile CO dissociation. Catalysis Communications, 2016, 77, 5-8. | 3.3 | 18 |
| 405 | Kinetic aspects of chain growth in Fischer–Tropsch synthesis. Faraday Discussions, 2017, 197, 153-164. | 3.2 | 18 |
| 406 | Confined Carbon Mediating Dehydroaromatization of Methane over Mo/ZSMâ€5. Angewandte Chemie, 2018, 130, 1028-1032. | 2.0 | 18 |
| 407 | N2O decomposition over Fe/ZSM-5: reversible generation of highly active cationic Fe species. Chemical Communications, 2002, , 1232-1233. | 4.1 | 17 |
| 408 | Intrinsic Thiophene Hydrodesulfurization Kinetics of a Sulfided NiMo/SiO2Model Catalyst: Volcano-Type Behavior. Catalysis Letters, 2003, 90, 117-122. | 2.6 | 17 |
| 409 | Cluster Model DFT Study of CO Adsorption to Gallium Ions in Ga/HZSM-5. Journal of Physical Chemistry C, 2008, 112, 3321-3326. | 3.1 | 17 |
| 410 | Glucose Dehydration to 5-Hydroxymethylfurfural by a Combination of a Basic Zirconosilicate and a Solid Acid. Catalysis Letters, 2014, 144, 2121-2128. | 2.6 | 17 |
| 411 | A DFT Study of CO ₂ Hydrogenation on Faujasiteâ€Supported Ir ₄ Clusters: on the Role of Water for Selectivity Control. ChemCatChem, 2016, 8, 2500-2507. | 3.7 | 17 |
| 412 | Instability of NiMoS ₂ and CoMoS ₂ Hydrodesulfurization Catalysts at Ambient Conditions: A Quasi in Situ High-Resolution Transmission Electron Microscopy and X-ray Photoelectron Spectroscopy Study. Journal of Physical Chemistry C, 2016, 120, 19204-19211. | 3.1 | 17 |
| 413 | Oriented Pt Nanoparticles Supported on Few-Layers Graphene as Highly Active Catalyst for Aqueous-Phase Reforming of Ethylene Glycol. ACS Applied Materials & Interfaces, 2016, 8, 33690-33696. | 8.0 | 17 |
| 414 | Eight-coordinate fluoride in a silicate double-four-ring. Proceedings of the National Academy of Sciences of the United States of America, 2017, 114, 828-833. | 7.1 | 17 |

| # | Article | IF | CITATIONS |
|-----|--|------|-----------|
| 415 | Cesium's Offâ€ŧheâ€Map Valence Orbital. Angewandte Chemie - International Edition, 2017, 56, 9772-9776. | 13.8 | 17 |
| 416 | CO2 and H2O chemisorption mechanism on different potassium-promoted sorbents for SEWGS processes. Journal of CO2 Utilization, 2018, 25, 180-193. | 6.8 | 17 |
| 417 | Hydrogenation of Lactic Acid to 1,2â€Propanediol over Ruâ€Based Catalysts. ChemCatChem, 2018, 10, 810-817. | 3.7 | 17 |
| 418 | Direct epoxidation of propene on silylated Au–Ti catalysts: a study on silylation procedures and the effect on propane formation. Catalysis Science and Technology, 2018, 8, 3052-3059. | 4.1 | 17 |
| 419 | Template-Free Nanostructured Fluorine-Doped Tin Oxide Scaffolds for Photoelectrochemical Water Splitting. ACS Applied Materials & Interfaces, 2019, 11, 36485-36496. | 8.0 | 17 |
| 420 | Shape selectivity in linear paraffins hydroconversion in 10-membered-ring pore zeolites. Journal of Catalysis, 2021, 394, 284-298. | 6.2 | 17 |
| 421 | The role of H2 in Fe carburization by CO in Fischer-Tropsch catalysts. Journal of Catalysis, 2021, 400, 93-102. | 6.2 | 17 |
| 422 | Epoxidation of propene using Au/TiO2: on the difference between H2 and CO as a co-reactant. Catalysis Science and Technology, 2017, 7, 2252-2261. | 4.1 | 16 |
| 423 | Early Transition Metal Doped Tungstite as an Effective Catalyst for Glucose Upgrading to 5-Hydroxymethylfurfural. Catalysis Letters, 2018, 148, 3093-3101. | 2.6 | 16 |
| 424 | Mild dealumination of template-stabilized zeolites by NH ₄ F. Catalysis Science and Technology, 2019, 9, 4239-4247. | 4.1 | 16 |
| 425 | Operando Spectroscopy Unveils the Catalytic Role of Different Palladium Oxidation States in CO Oxidation on Pd/CeO ₂ Catalysts. Angewandte Chemie - International Edition, 2022, 61, . | 13.8 | 16 |
| 426 | A computational study of the mechanism of CO oxidation by a ceria supported surface rhodium oxide layer. Chemical Communications, 2013, 49, 3851. | 4.1 | 15 |
| 427 | CO oxidation on Rh-doped hexadecagold clusters. Catalysis Science and Technology, 2017, 7, 75-83. | 4.1 | 15 |
| 428 | Highly active and stable spinel-oxide supported gold catalyst for gas-phase selective aerobic oxidation of cyclohexanol to cyclohexanone. Catalysis Communications, 2018, 117, 53-56. | 3.3 | 15 |
| 429 | A quantum-chemical study of the CO dissociation mechanism on low-index Miller planes of l̆-Fe3C. Catalysis Today, 2020, 342, 152-160. | 4.4 | 15 |
| 430 | The role of chromium in iron-based high-temperature water-gas shift catalysts under industrial conditions. Applied Catalysis B: Environmental, 2021, 297, 120465. | 20.2 | 15 |
| 431 | Polyamide Synthesis from 6-Aminocapronitrile, Part 2: Heterogeneously Catalyzed Nitrile Hydrolysis with Consecutive Amine Amidation. Chemistry - A European Journal, 2007, 13, 7673-7681. | 3.3 | 14 |
| 432 | Retro-analysis of silicate aggregation in pentasil zeolite formation. Catalysis Today, 2011, 169, 156-166. | 4.4 | 14 |

| # | Article | IF | CITATIONS |
|-----|---|------|-----------|
| 433 | New Cuâ€Based Catalysts Supported on TiO ₂ Films for Ullmann S _N Arâ€Type CO Coupling Reactions. Chemistry - A European Journal, 2012, 18, 1800-1810. | 3.3 | 14 |
| 434 | On the Formation of Cd–Zn Sulfide Photocatalysts from Insoluble Hydroxide Precursors. Inorganic Chemistry, 2015, 54, 9491-9498. | 4.0 | 14 |
| 435 | The nature of strong BrÃ,nsted acidity of Ni-SMM clay. Applied Catalysis B: Environmental, 2016, 191, 62-75. | 20.2 | 14 |
| 436 | On the origin of the photocurrent of electrochemically passivated p-InP(100) photoelectrodes. Physical Chemistry Chemical Physics, 2018, 20, 14242-14250. | 2.8 | 14 |
| 437 | Crystallographic orientation of facets and planar defects in functional nanostructures elucidated by nano-focused coherent diffractive X-ray imaging. Nanoscale, 2018, 10, 4833-4840. | 5.6 | 14 |
| 438 | Marrying SPR excitation and metal–support interactions: unravelling the contribution of active surface species in plasmonic catalysis. Nanoscale, 2018, 10, 8560-8568. | 5.6 | 14 |
| 439 | Mordenite Nanorods Prepared by an Inexpensive Pyrrolidineâ€based Mesoporogen for Alkane Hydroisomerization. ChemCatChem, 2019, 11, 2803-2811. | 3.7 | 14 |
| 440 | A Multiâ€Parametric Catalyst Screening for CO ₂ Hydrogenation to Ethanol. ChemCatChem, 2021, 13, 3324-3332. | 3.7 | 14 |
| 441 | Twin boundary migration in an individual platinum nanocrystal during catalytic CO oxidation. Nature Communications, 2021, 12, 5385. | 12.8 | 14 |
| 442 | Real-time dynamics and structures of supported subnanometer catalysts via multiscale simulations. Nature Communications, 2021, 12, 5430. | 12.8 | 14 |
| 443 | Concentration and temperature dependence of the diffusivity of n-hexane in MFI-zeolites. Microporous and Mesoporous Materials, 2005, 77, 119-129. | 4.4 | 13 |
| 444 | A DFT study on benzene adsorption over a corner site of tungsten sulfides. Catalysis Today, 2008, 130, 178-182. | 4.4 | 13 |
| 445 | Structure of palladium nanoparticles under oxidative conditions. Physical Chemistry Chemical Physics, 2015, 17, 2268-2273. | 2.8 | 13 |
| 446 | Bottlenecks limiting efficiency of photocatalytic water reduction by mixed Cd-Zn sulfides/Pt-TiO 2 composites. Applied Catalysis B: Environmental, 2016, 198, 16-24. | 20.2 | 13 |
| 447 | Effect of USY Zeolite Chemical Treatment with Ammonium Nitrate on Its VGO Hydrocracking Performance. Energy & Fuels, 2016, 30, 616-625. | 5.1 | 13 |
| 448 | Polypeptide Polymer Brushes by Lightâ€Induced Surface Polymerization of Amino Acid <i>N</i> arboxyanhydrides. Macromolecular Rapid Communications, 2018, 39, e1700743. | 3.9 | 13 |
| 449 | Assessment of the Location of Pt Nanoparticles in Pt/zeolite Y∫î³â€Al ₂ O ₃ Composite Catalysts. ChemCatChem, 2020, 12, 615-622. | 3.7 | 13 |
| 450 | Influence of hematite morphology on the CO oxidation performance of Au/α-Fe2O3. Chinese Journal of Catalysis, 2021, 42, 658-665. | 14.0 | 13 |

| # | Article | IF | CITATIONS |
|-----|--|------|-----------|
| 451 | Mechanistic study of catalytic CO ₂ hydrogenation in a plasma by operando DRIFT spectroscopy. Journal Physics D: Applied Physics, 2021, 54, 264004. | 2.8 | 13 |
| 452 | Studying Reaction Mechanisms in Solution Using a Distributed Electron Microscopy Method. ACS Nano, 2021, 15, 10296-10308. | 14.6 | 13 |
| 453 | Protection Strategies for the Conversion of Biobased Furanics to Chemical Building Blocks. ACS Sustainable Chemistry and Engineering, 2022, 10, 3116-3130. | 6.7 | 13 |
| 454 | A periodic density functional theory study of gallium-exchanged mordenite. Comptes Rendus Chimie, 2005, 8, 509-520. | 0.5 | 12 |
| 455 | A DFT Study of Hydrogen–deuterium Exchange over Oxidized and Reduced Gallium Species in Ga/HZSM-5 Zeolite. Catalysis Letters, 2006, 108, 187-191. | 2.6 | 12 |
| 456 | Microkinetic Modeling of the Oxygen Reduction Reaction at the Pt(111)/Gas Interface. Catalysis Letters, 2015, 145, 451-457. | 2.6 | 12 |
| 457 | A quantum-chemical DFT study of CO dissociation on Fe-promoted stepped Rh surfaces. Catalysis Today, 2016, 275, 111-118. | 4.4 | 12 |
| 458 | FT-IR study of NO adsorption on MoS2/Al2O3 hydrodesulfurization catalysts: Effect of catalyst preparation. Catalysis Today, 2017, 292, 67-73. | 4.4 | 12 |
| 459 | High pressure flow reactor for in situ X-ray absorption spectroscopy of catalysts in gas-liquid mixtures—A case study on gas and liquid phase activation of a Co-Mo/Al 2 O 3 hydrodesulfurization catalyst. Catalysis Today, 2017, 292, 51-57. | 4.4 | 12 |
| 460 | Investigating the role of the different metals in hydrotalcite Mg/Al-based adsorbents and their interaction with acidic sorbate species. Chemical Engineering Science, 2019, 200, 138-146. | 3.8 | 12 |
| 461 | Linear Activation Energy-Reaction Energy Relations for LaBO3 (B = Mn, Fe, Co, Ni) Supported Single-Atom Platinum Group Metal Catalysts for CO Oxidation. Journal of Physical Chemistry C, 2019, 123, 31130-31141. | 3.1 | 12 |
| 462 | Electrocatalytic synthesis of organic carbonates. Chemical Communications, 2020, 56, 13082-13092. | 4.1 | 12 |
| 463 | Renewable Thiol–yne "Click―Networks Based on Propargylated Lignin for Adhesive Resin Applications. ACS Applied Polymer Materials, 2022, 4, 2544-2552. | 4.4 | 12 |
| 464 | Sintering and carbidization under simulated high conversion on a cobalt-based Fischer-Tropsch catalyst; manganese oxide as a structural promotor. Journal of Catalysis, 2022, 413, 106-118. | 6.2 | 12 |
| 465 | Preparation, characterization and catalytic activity of non-hydrothermally synthesized saponite-like materials. Studies in Surface Science and Catalysis, 2002, 142, 271-278. | 1.5 | 11 |
| 466 | Silver addition to a cobalt Fischer–Tropsch catalyst. Journal of Catalysis, 2018, 366, 107-114. | 6.2 | 11 |
| 467 | The Impact of Biomass and Acid Loading on Methanolysis during Two-Step Lignin-First Processing of Birchwood. Catalysts, 2021, 11, 750. | 3.5 | 11 |
| 468 | Facile synthesis of nanosized mordenite and beta zeolites with improved catalytic performance: non-surfactant diquaternary ammonium compounds as structure-directing agents. Inorganic Chemistry Frontiers, 2022, 9, 3200-3216. | 6.0 | 11 |

| # | Article | IF | CITATIONS |
|-----|---|------|-----------|
| 469 | Imaging the facet surface strain state of supported multi-faceted Pt nanoparticles during reaction. Nature Communications, 2022, 13, . | 12.8 | 11 |
| 470 | Promotion of Thiophene Hydrodesulfurization by Ammonia over Amorphous-Silicaâ^'Alumina-Supported CoMo and NiMo Sulfides. Industrial & Engineering Chemistry Research, 2007, 46, 4202-4211. | 3.7 | 10 |
| 471 | Ionicâ€Liquidâ€Stabilized Rhodium Nanoparticles for Citral Cyclodehydration. ChemSusChem, 2010, 3, 1264-1267. | 6.8 | 10 |
| 472 | Adsorption of Argon on MFI Nanosheets: Experiments and Simulations. Journal of Physical Chemistry C, 2013, 117, 24503-24510. | 3.1 | 10 |
| 473 | Scaling-Up Catalytic Depolymerisation of Lignin: Performance Criteria for Industrial Operation. Topics in Catalysis, 2018, 61, 1901-1911. | 2.8 | 10 |
| 474 | <i>In situ</i> structural evolution of single particle model catalysts under ambient pressure reaction conditions. Nanoscale, 2019, 11, 331-338. | 5.6 | 10 |
| 475 | Insight into the Formation of Nanostructured MFI Sheets and MEL Needles Driven by Molecular Recognition. Journal of Physical Chemistry C, 2019, 123, 5326-5335. | 3.1 | 10 |
| 476 | Gas-phase selective oxidation of cyclohexanol to cyclohexanone over Au/Mg1-xCuxCr2O4 catalysts: On the role of Cu doping. Journal of Catalysis, 2020, 384, 218-230. | 6.2 | 10 |
| 477 | Low-temperature, atmospheric pressure reverse water-gas shift reaction in dielectric barrier plasma discharge, with outlook to use in relevant industrial processes. Chemical Engineering Science, 2020, 225, 115803. | 3.8 | 10 |
| 478 | lsotopic Exchange Study on the Kinetics of Fe Carburization and the Mechanism of the Fischer–Tropsch Reaction. ACS Catalysis, 2022, 12, 2877-2887. | 11.2 | 10 |
| 479 | Ammonia electrocatalytic synthesis from nitrate. Electrochemical Science Advances, 2023, 3, . | 2.8 | 10 |
| 480 | A DFT study on benzene adsorption over tungsten sulfides: surface model and adsorption geometries. Topics in Catalysis, 2007, 45, 175-179. | 2.8 | 9 |
| 481 | Structure and Basicity of Microporous Titanosilicate ETS-10 and Vanadium-Containing ETS-10. Journal of Physical Chemistry C, 2012, 116, 17124-17133. | 3.1 | 9 |
| 482 | Hierarchical fabrication of silica cocoon with hexagonally ordered channel constructed wall via an emulsion-assisted process. Microporous and Mesoporous Materials, 2012, 150, 90-95. | 4.4 | 9 |
| 483 | Effective Release of Lignin Fragments from Lignocellulose by Lewis Acid Metal Triflates in the Ligninâ€First Approach. ChemSusChem, 2016, 9, 3261-3261. | 6.8 | 9 |
| 484 | Preparative Aspects of Supported Ni2P Catalysts for Reductive Upgrading of Technical Lignin to Aromatics. Catalysis Letters, 2017, 147, 1722-1731. | 2.6 | 9 |
| 485 | Adsorption behavior and kinetics of H2S on a potassium-promoted hydrotalcite. International Journal of Hydrogen Energy, 2018, 43, 20758-20771. | 7.1 | 9 |
| 486 | 2D surface induced self-assembly of Pd nanocrystals into nanostrings for enhanced formic acid electrooxidation. Journal of Materials Chemistry A, 2020, 8, 17128-17135. | 10.3 | 9 |

| # | Article | IF | CITATIONS |
|-----|---|------|-----------|
| 487 | Subâ€Nanometer Confined Ions and Solvent Molecules Intercalation Capacitance in Microslits of 2D Materials. Small, 2021, 17, e2104649. | 10.0 | 9 |
| 488 | "Extracting―the Key Fragment in ETSâ€10 Crystallization and Its Application in AMâ€6 Assembly. Chemistry A European Journal, 2012, 18, 12078-12084. | 3.3 | 8 |
| 489 | Catalysis for Fuels: general discussion. Faraday Discussions, 2017, 197, 165-205. | 3.2 | 8 |
| 490 | Origin of enhanced BrÃ,nsted acidity of NiF-modified synthetic mica–montmorillonite clay. Catalysis Science and Technology, 2018, 8, 244-251. | 4.1 | 8 |
| 491 | Hierarchically Porous (Alumino)Silicates Prepared by an Imidazole-Based Surfactant and Their Application in Acid-Catalyzed Reactions. ACS Applied Materials & Interfaces, 2019, 11, 40151-40162. | 8.0 | 8 |
| 492 | Selective methanethiol-to-olefins conversion over HSSZ-13 zeolite. Chemical Communications, 2021, 57, 3323-3326. | 4.1 | 8 |
| 493 | Alkali catalyzes methanethiol synthesis from CO and H2S. Journal of Catalysis, 2022, 405, 116-128. | 6.2 | 8 |
| 494 | Insights into Supported Subnanometer Catalysts Exposed to CO <i>via</i> Machine-Learning-Enabled Multiscale Modeling. Chemistry of Materials, 2022, 34, 1611-1619. | 6.7 | 8 |
| 495 | Nonhydrothermal Synthesis and Properties of Saponite-Like Materials. Russian Journal of Applied Chemistry, 2003, 76, 700-705. | 0.5 | 7 |
| 496 | Modification of BrÃ,nsted acidity of zeolites by Ga+, GaO+ and AlO+: comparison for alkane activation. Studies in Surface Science and Catalysis, 2007, 170, 1182-1189. | 1.5 | 7 |
| 497 | Synchrotron based operando surface Xâ€ray scattering study towards structure–activity relationships of model electrocatalysts. ChemistrySelect, 2016, 1, 1104-1108. | 1.5 | 7 |
| 498 | Synthesis, Physicochemical Characterization, and Cytotoxicity Assessment of CeO ₂ Nanoparticles with Different Morphologies. European Journal of Inorganic Chemistry, 2017, 2017, 3184-3190. | 2.0 | 7 |
| 499 | Reactor for nano-focused x-ray diffraction and imaging under catalytic in situ conditions. Review of Scientific Instruments, 2017, 88, 093902. | 1.3 | 7 |
| 500 | Chemisorption of H2O and CO2 on Hydrotalcites for Sorption-enhanced Water-gas-Shift Processes. Energy Procedia, 2017, 114, 2228-2242. | 1.8 | 7 |
| 501 | The Influence and Removability of Colloidal Capping Agents on Carbon Monoxide Hydrogenation by Zirconiaâ€Supported Rhodium Nanoparticles. ChemCatChem, 2017, 9, 1018-1024. | 3.7 | 7 |
| 502 | Ligand-free ZnS nanoparticles: as easy and green as it gets. Chemical Communications, 2020, 56, 8707-8710. | 4.1 | 7 |
| 503 | Copper promotion of chromium-doped iron oxide water-gas shift catalysts under industrially relevant conditions. Journal of Catalysis, 2022, 405, 391-403. | 6.2 | 7 |
| 504 | Effective Oxidation of 5â€Hydroxymethylfurfural to 2,5â€Điformylfuran by an Acetal Protection Strategy. ChemSusChem, 2022, 15, . | 6.8 | 7 |

| # | Article | IF | CITATIONS |
|-----|--|------|-----------|
| 505 | Bifunctional Pt–Re Catalysts in Hydrodeoxygenation of Isoeugenol as a Model Compound for Renewable Jet Fuel Production. ACS Engineering Au, 2022, 2, 436-449. | 5.1 | 7 |
| 506 | Comment on "Efficient Conversion of Methane to Aromatics by Coupling Methylation Reaction― ACS Catalysis, 2017, 7, 4485-4487. | 11.2 | 6 |
| 507 | On Layered Silicates and Zeolitic Nanosheets. Angewandte Chemie - International Edition, 2017, 56, 5160-5163. | 13.8 | 6 |
| 508 | Efficient and Highly Transparent Ultraâ€Thin Nickelâ€Iron Oxyâ€hydroxide Catalyst for Oxygen Evolution Prepared by Successive Ionic Layer Adsorption and Reaction. ChemPhotoChem, 2019, 3, 1050-1054. | 3.0 | 6 |
| 509 | Stability of Colloidal Iron Oxide Nanoparticles on Titania and Silica Support. Chemistry of Materials, 2020, 32, 5226-5235. | 6.7 | 6 |
| 510 | Reversible hydrogenation restores defected graphene to graphene. Science China Chemistry, 2021, 64, 1047-1056. | 8.2 | 6 |
| 511 | Research Trends in FischerTropsch Catalysis for Coal to Liquids Technology. Frontiers of Engineering Management, 2016, 3, 321. | 6.1 | 6 |
| 512 | Synthesis of Nanocrystalline Mordenite Zeolite with Improved Performance in Benzene Alkylation and nâ€Paraffins Hydroconversion. ChemCatChem, 2022, 14, . | 3.7 | 6 |
| 513 | A Catalytic Strategy for Selective Production of 5â€Formylfuranâ€2â€carboxylic Acid and Furanâ€2,5â€dicarboxylic Acid. ChemCatChem, 2022, 14, . | 3.7 | 6 |
| 514 | Influence of the size, order and topology of mesopores in bifunctional Pd-containing acidic SBA-15 and M41S catalysts for n-hexadecane hydrocracking. Fuel Processing Technology, 2022, 232, 107259. | 7.2 | 6 |
| 515 | Cobalt–molybdenum-sulfide particles inside NaY zeolite?. Applied Catalysis A: General, 2002, 236, 205-222. | 4.3 | 5 |
| 516 | DFT Study on mechanochemical bond breaking in COGEF and Molecular Dynamics simulations. Procedia Computer Science, 2011, 4, 1167-1176. | 2.0 | 5 |
| 517 | Inside Cover: Molecular Aspects of Glucose Dehydration by Chromium Chlorides in Ionic Liquids (Chem. Eur. J. 19/2011). Chemistry - A European Journal, 2011, 17, 5210-5210. | 3.3 | 5 |
| 518 | Bent Carbon Surface Moieties as Active Sites on Carbon Catalysts for Phosgene Synthesis. Angewandte Chemie, 2016, 128, 1760-1764. | 2.0 | 5 |
| 519 | Molecular weight-based fractionation of lignin oils by membrane separation technology. Holzforschung, 2020, 74, 166-174. | 1.9 | 5 |
| 520 | A theoretical study of CO oxidation and O2 activation for transition metal overlayers on SrTiO3 perovskite. Journal of Catalysis, 2020, 391, 229-240. | 6.2 | 5 |
| 521 | Cu Electrodeposition on Nanostructured MoS ₂ and WS ₂ and Implications for HER Active Site Determination. Journal of the Electrochemical Society, 2020, 167, 116517. | 2.9 | 5 |
| 522 | Lateral Interactions of Dynamic Adlayer Structures from Artificial Neural Networks. Journal of Physical Chemistry C, 2022, 126, 5529-5540. | 3.1 | 5 |

| # | Article | IF | CITATIONS |
|-----|--|------|-----------|
| 523 | The application of non-hydrothermally prepared stevensites as support for hydrodesulfurization catalysts. Studies in Surface Science and Catalysis, 2000, , 257-265. | 1.5 | 4 |
| 524 | Influence of preparation procedure on the surface chemistry and catalytic characteristics of FeZSM-5 zeolite in selective oxidation of benzene to phenol. Russian Journal of Applied Chemistry, 2006, 79, 1115-1121. | 0.5 | 4 |
| 525 | Direct and NO-assisted N2O decomposition over Cu-zeolites. Studies in Surface Science and Catalysis, 2007, 170, 1080-1087. | 1.5 | 4 |
| 526 | Positron Emission Profiling: aÂStudy of Hydrocarbon Diffusivity in MFI Zeolites. Molecular Sieves - Science and Technology, 2007, , 277-328. | 0.2 | 4 |
| 527 | Effect of pressure on the sulfidation behavior of NiW catalysts: A 182W Mössbauer spectroscopy study. Catalysis Today, 2010, 150, 224-230. | 4.4 | 4 |
| 528 | Size dependence of photocatalytic oxidation reactions of Rh nanoparticles dispersed on (Ga1-xZnx)(N1-xOx) support. Chinese Journal of Catalysis, 2014, 35, 1944-1954. | 14.0 | 4 |
| 529 | Gold Clusters and Nanoparticles Stabilized by Nanoshaped Ceria in Catalysis. , 2015, , 99-132. | | 4 |
| 530 | Tracking Local Mechanical Impact in Heterogeneous Polymers with Direct Optical Imaging. Angewandte Chemie, 2018, 130, 16623-16628. | 2.0 | 4 |
| 531 | Reversible Nature of Coke Formation on Mo/ZSMâ€5 Methane Dehydroaromatization Catalysts. Angewandte Chemie, 2019, 131, 7142-7146. | 2.0 | 4 |
| 532 | A versatile mono-quaternary ammonium salt as a mesoporogen for the synthesis of hierarchical zeolites. Catalysis Science and Technology, 2019, 9, 6737-6748. | 4.1 | 4 |
| 533 | A novel semi-batch autoclave reactor to overcome thermal dwell time in solvent liquefaction experiments. Chemical Engineering Journal, 2021, 417, 128074. | 12.7 | 4 |
| 534 | Heterogeneous catalysts for the non-oxidative conversion of methane to aromatics and olefins. , 2021, , . | | 4 |
| 535 | Facetâ€Dependent Strain Determination in Electrochemically Synthetized Platinum Model Catalytic Nanoparticles. Small, 2021, 17, e2007702. | 10.0 | 4 |
| 536 | A scanning pulse reaction technique for transient analysis of the methanol-to-hydrocarbons reaction. Catalysis Today, 2023, 417, 113740. | 4.4 | 4 |
| 537 | Modification of inorganic supports with nickel acetylacetonate: The effect of their surface properties. Kinetics and Catalysis, 2006, 47, 451-459. | 1.0 | 3 |
| 538 | The origin of isotope-induced helical-sense bias in supramolecular polymers of benzene-1,3,5-tricarboxamides. Physical Chemistry Chemical Physics, 2012, 14, 13997. | 2.8 | 3 |
| 539 | Computational Chemistry of Zeolite Catalysis. , 2016, , 111-135. | | 3 |
| 540 | Graphene as Metalâ€Free Catalyst for Aqueous Phase Reforming of Ethylene Glycol. ChemistrySelect, 2017, 2, 6338-6343. | 1.5 | 3 |

| # | Article | IF | CITATIONS |
|-----|--|------|-----------|
| 541 | Lewis Acid Catalysis by Zeolites * *These authors contributed equally , 2018, , 229-263. | | 3 |
| 542 | The Important Role of Rubidium Hydroxide in the Synthesis of Hierarchical ZSM-5 Zeolite Using Cetyltrimethylammonium as Structure-Directing Agent. European Journal of Inorganic Chemistry, 2019, 2019, 2493-2497. | 2.0 | 3 |
| 543 | Role of bismuth on aerobic benzyl alcohol oxidation over ceria polymorph-supported gold nanoparticles. Catalysis Communications, 2020, 140, 106004. | 3.3 | 3 |
| 544 | Investigation of the combustion and emissions of ligninâ€derived aromatic oxygenates in a marine diesel engine. Biofuels, Bioproducts and Biorefining, 2021, 15, 1709. | 3.7 | 3 |
| 545 | Influence of polyvinylpyrrolidone as stabilizing agent on Pt nanoparticles in Pt/H-BEA catalyzed hydroconversion of n-hexadecane. Fuel, 2022, 317, 123506. | 6.4 | 3 |
| 546 | Amorphous Silicaâ€Alumina as Suitable Catalyst for the Dielsâ€Alder Cycloaddition of <i>2,5</i> â€Ðimethylfuran and Ethylene to Biobased <i>p</i> â€Xylene. ChemCatChem, 2022, 14, . | 3.7 | 3 |
| 547 | Zeolite Catalysis for Biomass Conversion. Green Chemistry and Sustainable Technology, 2016, , 347-372. | 0.7 | 2 |
| 548 | The Origin of High Activity of Amorphous MoS 2 in the Hydrogen Evolution Reaction. ChemSusChem, 2019, 12, 4336-4336. | 6.8 | 2 |
| 549 | Catalytic Conversion of Lignocellulosic Biomass:Application of Heterogeneous and Homogeneous Catalysts to Process Biomass into Value-Added Compounds. ACS Symposium Series, 2020, , 151-182. | 0.5 | 2 |
| 550 | A bifunctional catalyst based on Nb and V oxides over alumina: oxidative cleavage of crude glycerol to green formic acid. New Journal of Chemistry, 2020, 44, 8538-8544. | 2.8 | 2 |
| 551 | H2â^'D2 exchange and migration of Ga in H-ZSM5 and H-MOR zeolites. Studies in Surface Science and Catalysis, 2002, 142, 959-966. | 1.5 | 1 |
| 552 | A Combined Experimental and Computational Study of Alkane Activation over Ga+, GaO+, GaH2+ and H+ Ions in ZSM-5. Studies in Surface Science and Catalysis, 2007, , 417-420. | 1.5 | 1 |
| 553 | Chemistry and Reactivity of Transition Metal Sulphides in Relation to Their Catalytic Performance. , 1998, , 169-188. | | 1 |
| 554 | Synthesis of Stable and Low-CO ₂ Selective Phase-Pure ε-Iron Carbide Catalysts in Synthesis Gas Conversion. ACS Symposium Series, 2020, , 229-255. | 0.5 | 1 |
| 555 | Subâ€Nanometer Confined Ions and Solvent Molecules Intercalation Capacitance in Microslits of 2D Materials (Small 49/2021). Small, 2021, 17, . | 10.0 | 1 |
| 556 | Selective hydrogen oxidation in a mixture with ethane/ethene using Ce0.6Zr0.4O2 mixed oxides. Chemie-Ingenieur-Technik, 2001, 73, 766-766. | 0.8 | 0 |
| 557 | A Quasi In Situ HRTEM Study of the Air Stability of (Ni/Co)MoS2 Hydrodesulfurization Catalysts. Microscopy and Microanalysis, 2015, 21, 801-802. | 0.4 | 0 |
| 558 | Photoelectrochemistry: Enhanced Photoresponse of FeS2 Films: The Role of Marcasite-Pyrite Phase Junctions (Adv. Mater. 43/2016). Advanced Materials, 2016, 28, 9656-9656. | 21.0 | 0 |

| # | Article | IF | CITATIONS |
|-----|---|-------------------|------------|
| 559 | Computational Chemistry of Catalytic Biomass Conversion. Green Chemistry and Sustainable Technology, 2016, , 63-104. | 0.7 | 0 |
| 560 | Innenrücktitelbild: Nonâ€Pincerâ€Type Manganese Complexes as Efficient Catalysts for the Hydrogenation of Esters (Angew. Chem. 26/2017). Angewandte Chemie, 2017, 129, 7787-7787. | 2.0 | 0 |
| 561 | Heterogeneous Catalysis. , 2017, , 15-71. | | 0 |
| 562 | Innentitelbild: Confined Carbon Mediating Dehydroaromatization of Methane over Mo/ZSMâ€5 (Angew.) Tj ETQq | 0 0 0 rgBT 2.0 | Overlock 1 |
| 563 | Mordenite Nanorods Prepared by an Inexpensive Pyrrolidineâ€based Mesoporogen for Alkane Hydroisomerization. ChemCatChem, 2019, 11, 2754-2754. | 3.7 | 0 |
| 564 | Reply to: "Pitfalls in identifying active catalyst species― Nature Communications, 2020, 11, 4574. | 12.8 | 0 |
| 565 | Metal-support interfaces in ceria-based catalysts. , 2021, , . | | 0 |

566Positron Emission Profiling â€" The Ammonia Oxidation Reaction as a Case Study. Catalytic Science0.00567Series, 2006, , 213-260.0.00

567Operando Spectroscopy Unveils the Catalytic Role of Different Palladium Oxidation States in CO
Oxidation on Pd/CeO ₂ Catalysts. Angewandte Chemie, 0, , .2.00

Titelbild: Operando Spectroscopy Unveils the Catalytic Role of Different Palladium Oxidation States in568CO Oxidation on Pd/CeO₂ Catalysts (Angew. Chem. 23/2022). Angewandte Chemie, 2022, 134,2.00

.